

Models of c -axis twist Josephson tunneling

A. Bille,¹ R. A. Klemm,^{2,3,*} and K. Scharnberg¹

¹*I. Institut für Theoretische Physik, Universität Hamburg, Jungiusstraße 9, D-20355 Hamburg, Germany*

²*Max-Planck-Institut für Physik komplexer Systeme, Nöthnitzer Straße 38, D-01187 Dresden, Germany*

³*Materials Science Division, Argonne National Laboratory, Argonne, Illinois 60439*

(Received 17 May 2000; revised manuscript received 5 March 2001; published 9 October 2001)

We calculate the critical current density $J_c^J(\phi_0)$ for Josephson tunneling between identical high-temperature superconductors twisted an angle ϕ_0 about the c axis. Regardless of the shape of the two-dimensional Fermi surface and for very general tunneling matrix elements, an order parameter (OP) with general d -wave symmetry leads to $J_c^J(\pi/4) = 0$. This general result is inconsistent with the data of Li *et al.* [Phys. Rev. Lett. **83**, 4160 (1999)] on $\text{Bi}_2\text{Sr}_2\text{CaCu}_2\text{O}_{8+\delta}$ (Bi2212), which showed J_c^J to be independent of ϕ_0 . If the momentum parallel to the barrier is conserved in the tunneling process, J_c^J should vary substantially with the twist angle ϕ_0 when the tight-binding Fermi surface appropriate for Bi2212 is taken into account, even if the OP is completely isotropic. We quantify the degree of momentum nonconservation necessary to render $J_c^J(\phi_0)$ constant within experimental error for a variety of pair states by interpolating between the coherent and incoherent limits using five specific models to describe the momentum dependence of the tunneling matrix element squared. From the data of Li *et al.*, we conclude that the c -axis tunneling in Bi2212 must be very nearly incoherent, and that the OP must have a nonvanishing Fermi-surface average for $T \leq T_c$. We further show that the apparent conventional sum-rule violation observed by Basov *et al.* [Science **283**, 49 (1999)] can be consistent with such strongly incoherent c -axis tunneling.

DOI: 10.1103/PhysRevB.64.174507

PACS number(s): 74.72.Hs, 74.50.+r, 74.80.Dm, 74.60.Jg

I. INTRODUCTION

There is still considerable interest in the symmetry of the order parameter (OP) in the high-temperature superconductors (HTSC).^{1–11} Although many phase-sensitive experiments were interpreted as giving evidence for an OP in $\text{YBa}_2\text{Cu}_3\text{O}_{7-\delta}$ (YBCO) consistent with the $d_{x^2-y^2}$ -wave form,^{1,2} it is only recently that the same type of phase-sensitive experiments on the electron-doped HTSC $\text{Nd}_{1.85}\text{Ce}_{0.15}\text{CuO}_{4-y}$ (NCCO) and $\text{Pr}_{1.85}\text{Ce}_{0.15}\text{CuO}_{4-y}$ (PCCO) were also interpreted in terms of a $d_{x^2-y^2}$ -wave OP,³ possibly in agreement with penetration depth measurements,^{4,5} although those experiments could only place upper limits upon the gap minimum. However, the zero-bias conductance peak, often associated with Andreev bound states for tunneling into certain directions of a $d_{x^2-y^2}$ superconductor, was usually absent in NCCO and PCCO.⁵ The presence or absence of such peaks in YBCO is very sensitive to the surface properties, especially to the oxygen doping.⁶ Furthermore, the recent nonlinear transverse magnetization experiment on YBCO provided a minimum value of the superconducting gap, inconsistent with the scenario of a dominant $d_{x^2-y^2}$ component of a mixed $s+d_{x^2-y^2}$ -wave OP.⁷

An older pair of experiments with superconducting quantum-interference device (SQUID)-like devices with Pb or Nb around a corner of YBCO^{12,13} involved extrapolation of either the critical current or the voltage to zero. In the latter case, it also involved fitting a sharp, delta-function-like peak to a sine wave. However, detailed studies on thin films demonstrated conclusively that both of those extrapolations were unreliable.¹⁴ A subsequent experiment involving Pb junctions straddling a corner of a YBCO single crystal,¹⁵ while suggestive of a π junction arising from a predominant

$d_{x^2-y^2}$ -wave OP, was explainable in terms of trapped flux lying within the layers and pinned at the corners,¹⁶ as has been directly observed in related materials using a scanning SQUID microscope.¹⁷ This situation maps precisely into the case of a monopole vortex at the center of a conventional superconducting-normal-superconducting junction, resulting in a node in the center of the “Fraunhofer” $I_c(B)$ pattern.¹⁸ In addition, an interesting YBCO/Pb SQUID configuration,¹⁹ while suggestive of $d_{x^2-y^2}$ -wave OP symmetry, was subsequently found to depend upon the details of the junction fabrication in a manner inconsistent with that analysis.²⁰

Phase-sensitive experiments on $\text{Bi}_2\text{Sr}_2\text{CaCu}_2\text{O}_{8+\delta}$ (Bi2212) gave strong evidence that the OP has a nonvanishing Fermi-surface average.^{8–10,21} First, c -axis Josephson tunneling between Bi2212 and either Pb or Nb demonstrated that the OP has a nonvanishing Fermi-surface average in Bi2212 below their respective transition temperature T_c values.^{9,10} Although the magnitude of $I_c R_n$ was found to be very small (a few microvolts), such values were also seen with Josephson junctions between Pb and the c axis of single-crystal NCCO and thin films of YBCO.^{11,22} Since untwinned single crystals of YBCO gave much larger c -axis $I_c R_n$ values, these low values might arise from materials problems at the Bi2212/Pb interface, as was suggested for NCCO/Pb junctions.¹¹ In fact, the T_c values of the Bi2212 layers at the Pb interface were generally suppressed by more than a factor of 2 from the bulk values.⁹

Second, c -axis tunneling across the junctions of Bi2212 intercalated with HgBr_2 has been studied using mesas.^{21,23} In these experiments, increasing the c -axis spacing by 6.3 Å increased the normal-state resistivity by a factor of 200. In the superconducting state, R_n and I_c changed by comparable factors, but their product $I_c R_n \approx 10$ mV was about half the optimal value expected in the Ambegaokar-Baratoff model of

purely incoherent c -axis tunneling between identical, isotropic s -wave superconductors.^{21,24} Such behavior is very difficult to understand in terms of a $d_{x^2-y^2}$ -wave OP.²⁵ Moreover, these conventionally large $I_c R_n$ values measured between extremely weak tunnel junctions interior to the crystal strongly suggest the dominant OP is s wave and the tunneling is incoherent.

Also, recent experiments on Nb Josephson-junction arrays have provided an explanation not only of the paramagnetic Meissner effect, sometimes observed in ceramic Bi2212 samples,²⁶ but also of spontaneous flux generation itself, not necessarily proportional to an integral multiple of the flux quantum Φ_0 , when three or more conventional Josephson junctions in a loop are present.²⁷ Combined with the fact that it is often very difficult to determine precisely over how large a region away from a vortex core one has to integrate the field using a SQUID microscope in order to obtain the correct value of the trapped flux,²⁸ such spontaneous, nonintegral flux generation with three junctions in a ring might provide an alternative explanation of the IBM tricrystal experiment.¹

The critical current $I_c(\phi)$ through YBCO in-plane (001)-tilt bicrystalline grain-boundary junctions has been found to decrease exponentially as the misorientation angle ϕ is varied from 10° to 45° in a number of experiments (see Refs. 29 and 30 and references therein). In experiments on thin films prepared by vapor phase epitaxy, a decrease in $I_c R_n$ with increasing ϕ is usually observed. This has been interpreted as evidence for d -wave pairing, as d -wave effects would reduce I_c with increasing ϕ without affecting R_n .³⁰ However, I_c and R_n across in-plane YBCO grain boundaries obtained from bulk bicrystal seed growths, which were shown by electron microscopy studies to be much straighter than the usual thin-film grain boundaries, varied inversely with ϕ , such that $I_c R_n$ remained constant ($\approx 12 \mu\text{V}$), even as $\phi \rightarrow 45^\circ$!²⁹ These $I_c R_n$ values are much smaller than measured on thin-film samples, but there the values depend upon the critical current and the substrate, which seems to indicate that one is not measuring intrinsic properties of the superconducting state. Curiously, the small $I_c R_n$ values measured in these greatly improved junctions are comparable to those obtained in c -axis tunneling between Pb and Bi2212, NCCO, and heavily twinned thin films of YBCO.^{9,11,22}

Furthermore, very high-quality (100)|(110) in-plane grain-boundary junctions were prepared by liquid phase epitaxy, and some of these junctions gave rise to a standard Fraunhofer diffraction pattern upon application of a parallel magnetic field near T_c .³¹ Such an observation is also easy to understand from incoherent tunneling with s -wave superconductivity, but is very difficult to explain with $d_{x^2-y^2}$ -wave superconductivity.³² Since the IBM tricrystal experiments were always performed on samples prepared by the older vapor phase deposition technique, the grain boundaries meandered greatly, and did not show the constant $I_c R_n$ behavior.²⁹ Thus, defects in the grain boundaries and the influence of the substrate might provide a second possible explanation of the IBM tricrystal experiment.

In addition, the temperature T and magnetic-field H dependencies of the intrinsic tunneling in such Bi2212 and

(HgBr₂)Bi2212 mesas have been reported, providing compelling evidence that the pseudogap and the superconducting gap or gaplike density-of-states features are completely unrelated to one another.²³ This independence of the pseudogap and superconducting state is also evident in the NMR $1/(T_1 T)$ measurements as a function of T and H , with the results being strongly H dependent below T_c , but completely independent of H above T_c in optimally and underdoped YBCO samples.^{33,34} Similar conclusions were attained using ultrafast optical relaxation measurements, in which the superconducting gap in YBCO was also found to be s wave near T_c .³⁵

The resonant peak observed in neutron scattering, previously thought to arise upon entry into a $d_{x^2-y^2}$ superconducting state, has recently been confirmed to be stabilized by impurities which themselves destroy the superconductivity.³⁶ Thus, this experiment, if phase sensitive, is apparently sensitive to the phase of the ordering responsible for the pseudogap, such as charge- and/or spin-density wave formation, rather than to the superconducting OP itself.³⁷ Hence, experiments such as photoemission, neutron scattering, and low-temperature thermodynamic and transport phenomena, etc., which can be influenced by the nonsuperconducting (e.g., density wave) ordering responsible for the pseudogap, are unreliable tests of the OP symmetry.

More directly, a phase-sensitive experiment which can test the symmetry of the OP over the entire range $T \leq T_c$ was performed.⁸ In this experiment, a single crystal of Bi2212 was cleaved in the ab plane, and the two cleaves were twisted in a chosen angle ϕ_0 about the c axis with respect to each other, and fused back together. Various experimental probes, including high-resolution TEM, confirmed that the bicrystal junctions were of exceptionally good quality.³⁸ In particular, atomic-scale steps that are known to be created during cleavage apparently completely disappear during the high-temperature sintering process, so that any significant contribution from tunneling in the ab direction can be ruled out. After lead attachment, the critical currents $I_c^J(T)$ and $I_c^S(T)$ across the twist junction and single crystals were measured, as were the respective junction areas A^J and A^S . For 11 of the 12 twist junctions measured, the resulting critical current densities $J_c^J(T)$ and $J_c^S(T)$ were the same at $T/T_c = 0.9$, independent of ϕ_0 .⁸ Since $J_c^J(\phi_0)/J_c^S = 1$ applies both to several samples at 45° and several a few degrees away from 45° , the tunneling at the twist junction is not due to any defects other than those naturally present within an untwisted single crystal. Li *et al.* claimed that (a) the intrinsic junctions and the twist junction behaved identically, (b) the c -axis tunneling is strongly incoherent, and (c) the OP contains an isotropic component, but not any purported $d_{x^2-y^2}$ -wave component for $T < T_c$, except possibly below a second, unobserved phase transition.⁸

Since then, the group-theoretic arguments upon which conclusion (c) were based have been published.⁴⁰ In addition, an exact calculation of the possible roles of coherent c -axis tunneling was published.⁴¹ For the tight-binding Fermi surface generally thought to be applicable to Bi2212,^{42,43} it was shown that such coherent tunneling was inconsistent

with the data,⁸ even for an isotropic s -wave OP. Since the claim (a) of Li *et al.* is just a statement of their experimental observations, and the claim (b) is clearly correct in the limit of purely incoherent tunneling, it remains to quantify precisely just how incoherent the tunneling must be in order to fit the data.

There have been earlier measurements of (001) twist boundaries in sintered Bi2212 bicrystals.³⁹ In those experiments, there seem to have been severe problems with junction quality, since most of the junction T_c values differed substantially from their respective bulk values. Accordingly, the measured J_c^J values varied unsystematically with ϕ_0 . For one sample with $\phi_0=36^\circ$, however, for which the junction T_c was almost identical to the bulk value, J_c^J (4.2 K) was found to be 40 A/cm², close to the value of 50 A/cm² measured on the reference sample with $\phi_0=2^\circ$. Even if J_c^J of the reference sample was suppressed and we were to take $J_c^J(4.2\text{ K})\approx 100\text{ A/cm}^2$, as observed by Li *et al.*,⁸ J_c^J for the 36° sample would be incompatible with the predictions of the d -wave model.

In a recent review article,¹ Tsuei, Kirtley, *et al.*, while briefly addressing c -axis twist junctions, quoted a large number of papers in support of the view that momentum-non-conserving (e.g., incoherent) processes should be included when discussing c -axis transport. They then conclude that such processes would reduce any sensitivity of the junction critical current density to the twist angle ϕ_0 . However, as shown in the following, such a conclusion applies only to pair states with s -wave symmetry. To make this quite clear, in Sec. II, we proved a theorem about the vanishing of the c -axis critical current for a 45° twist junction between d -wave superconductors, which is valid for a very general momentum dependence of the tunneling matrix element squared. For a d -wave superconductor, the critical current becomes insensitive to ϕ_0 only in the sense that it is zero for all ϕ_0 values in the extreme limit of incoherent tunneling. In Sec. IV, we show analytically for a general Fermi surface of tetragonal symmetry that the critical current density between d -wave superconductors, normalized to its $\phi_0=0$ value, varies as $\cos(2\phi_0)$ as the incoherent limit is approached, almost independently of the chosen model for the tunneling matrix element squared, and of the particular form of the d -wave OP.

We remark that although the c -axis twist experiments of Li *et al.* have not yet been fully reproduced in a second laboratory, neither have the tricrystal experiments of Tsuei, Kirtley *et al.*^{1,8} However, it is expected that within the next year or two, serious attempts to reproduce and extend both experiments will have been made. We would like to see c -axis twist experiments performed on small mesas containing a twist junction, to test the robustness of the scaling of the critical current with the junction area. With small mesas, one could also see the Fraunhofer diffraction pattern characteristic of each junction in the mesa, and could measure R_n for the total number of junctions in the mesa. In addition, we would like to see the IBM tricrystal experiment reproduced using c -axis twist junctions, as we suggested previously.⁴⁰

In the meantime, since the question of the symmetry of

the OP is by no means settled, it is very important that as many calculations intended to aid in our understanding of these important experimental results be presented. To date, the only published theories of this twist experiment did not explain it quantitatively,^{40,41} except for the unlikely case of a circular intralayer Fermi-surface cross section and very strong coherent interlayer intrinsic tunneling, leading to unreasonably isotropic normal-state behavior of Bi2212.⁴¹ Here we present and solve five tunneling models and several OP models which can actually fit the data quantitatively, using parameters appropriate for Bi2212.

II. GENERAL CONSIDERATIONS

Since Bi2212 behaves as a stack of weakly coupled Josephson junctions,⁴⁴ the static critical current density J_c across each junction may be evaluated by neglecting the couplings between the other junctions.^{8,40} Specifically, J_c^J across the twist junction between adjacent layers is given for $\hbar=c=k_B=1$ by

$$J_c^J(\phi_0) = \left| 4eT \sum_{\omega} \langle f^J(\mathbf{k}, \mathbf{k}') F_{\omega}(\mathbf{k}) F_{\omega}^{\dagger}(\tilde{\mathbf{k}}') \rangle \right|, \quad (1)$$

where e is the electronic charge, ω represents the Matsubara frequencies, $f^J(\mathbf{k}, \mathbf{k}')$ is the spatial average over the junction area of the tunneling matrix element squared,⁴⁰ $\langle \dots \rangle$ represents two-dimensional integrals over each of the two first Brillouin zones (BZ's), and the wave-vector $\tilde{\mathbf{k}}'$ is obtained from $\mathbf{k}' = (k'_x, k'_y)$ by a rotation of ϕ_0 about the c axis. The anomalous Green's functions are $F_{\omega}(\mathbf{k}) = \Delta(\mathbf{k}, T) / [\omega^2 + \xi^2(\mathbf{k}) + |\Delta(\mathbf{k}, T)|^2]$ and $F_{\omega}^{\dagger} = F_{\omega}^*$, where $\Delta(\mathbf{k}, T)$ and $\xi(\mathbf{k})$ are the OP and quasiparticle dispersion on the layer with wave vector \mathbf{k} , respectively. Since J_c^J is proportional to the magnitude of the maximum supercurrent, the relative phases of the OP's of each side of the junction can be ignored, so that $F_{\omega}^{\dagger}(\mathbf{k})$ can be replaced by $F_{\omega}(\mathbf{k})$. For Bi2212, we assume the quasiparticle dispersion $\xi(\mathbf{k})$ has the tight-binding form,

$$\xi(\mathbf{k}) = -t[\cos(k_x a) + \cos(k_y a)] + t' \cos(k_x a) \cos(k_y a) - \mu, \quad (2)$$

where we take $t=306\text{ meV}$, $t'/t=0.90$, and $\mu/t=-0.675$ to give a good fit to the Fermi surface of Bi2212, for which $\xi(\mathbf{k}_F)=0$. These values are slightly different from those used previously.⁴⁵ A plot of this Fermi surface is shown in Fig. 1.

We first consider a general $d_{x^2-y^2}$ - or d_{xy} -wave OP, which is odd under $\pi/2$ rotations about the c axis.⁴⁰ Let $R_{\mathbf{k}'}(\phi_0)$ be a rotation about the c axis by the angle ϕ_0 of the wave vector \mathbf{k}' , so that $F_{\omega}(\tilde{\mathbf{k}}') = R_{\mathbf{k}'}(\phi_0) F_{\omega}(\mathbf{k}')$. Then $R_{\mathbf{k}}(-\pi/4) F_{\omega}(\mathbf{k}) = -R_{\mathbf{k}}(\pi/4) F_{\omega}(\mathbf{k})$ for a general $d_{x^2-y^2}$ -wave (or general d_{xy} -wave) OP and a quasiparticle dispersion $\xi(\mathbf{k})$ that exhibits tetragonal symmetry, as in Eq. (2). This crucial point only applies for a $\pi/4$ rotation, since for $\phi_0 \neq \pi/4$, $R_{\mathbf{k}}(-\phi_0) F_{\omega}(\mathbf{k}) \neq -R_{\mathbf{k}}(\phi_0) F_{\omega}(\mathbf{k})$. Then, the critical current $J_{c,d}^J(\pi/4)$ across a 45° c -axis twist junction in

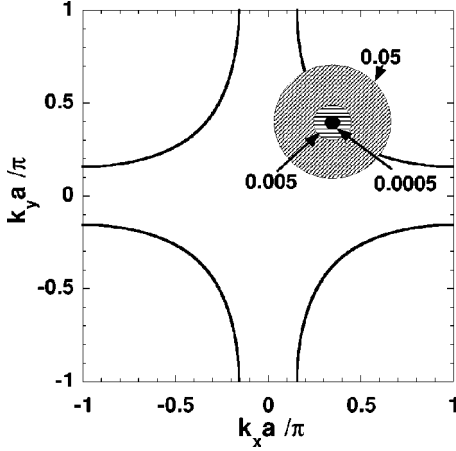


FIG. 1. Schematic plot of the Bi2212 Fermi surface used in these calculations. The concentric circles represent the portions of the BZ for which the tunneling strength is within $1/e$ for the Gaussian and exponential models ($1/2$ for the rotationally invariant Lorentzian and extended Lorentzian models) of its maximum value, for dimensionless parameters σ^2 of magnitudes 0.0005, 0.005, and 0.05, as indicated.

a tetragonal layered superconductor with a general $d_{x^2-y^2}$ - or d_{xy} -wave OP at an arbitrary $T \leq T_c$, to leading order in the tunneling strength, satisfies

$$J_{c,d}^J(\pi/4) = \left| 4eT \sum_{\omega} Q_{\omega} \right|, \quad (3)$$

where

$$Q_{\omega} = \langle f^J(\mathbf{k}, \mathbf{k}') [R_{\mathbf{k}'}(\pi/4) F_{\omega}(\mathbf{k}')] F_{\omega}(\mathbf{k}) \rangle \\ = \langle f^J(\mathbf{k}, \mathbf{k}') F_{\omega}(\mathbf{k}') [R_{\mathbf{k}}(-\pi/4) F_{\omega}(\mathbf{k})] \rangle \quad (4)$$

$$= \langle f^J(\mathbf{k}, \mathbf{k}') F_{\omega}(\mathbf{k}') [-R_{\mathbf{k}}(\pi/4) F_{\omega}(\mathbf{k})] \rangle \quad (5)$$

$$= \langle f^J(\mathbf{k}', \mathbf{k}) F_{\omega}(\mathbf{k}) [-R_{\mathbf{k}'}(\pi/4) F_{\omega}(\mathbf{k}')] \rangle \quad (6)$$

$$= -Q_{\omega} = 0. \quad (7)$$

In the above, we assumed $f^J(\mathbf{k}, \mathbf{k}') = f^J(\mathbf{k}', \mathbf{k})$. In the next-to-last step, we merely changed the integration variables. Thus, we have proven the general theorem that for any weak tunneling matrix element squared satisfying $f^J(\mathbf{k}, \mathbf{k}') = f^J(\mathbf{k}', \mathbf{k})$, an arbitrary OP of general $d_{x^2-y^2}$ - or d_{xy} -wave symmetry in a tetragonal crystal gives rise to a *vanishing* c -axis critical current across an internal 45° twist junction for $T \leq T_c$. The only requirements for this theorem to hold are (1) $f^J(\mathbf{k}, \mathbf{k}') = f^J(\mathbf{k}', \mathbf{k})$, which is a consequence of time-reversal invariance, (2) the tunneling is sufficiently weak that higher-order tunneling processes can be neglected, which is certainly the case for Bi2212,⁴⁴ (3) the crystal is tetragonal, and (4) the OP has either pure d_{xy} - or pure $d_{x^2-y^2}$ -wave symmetry. If these criteria are satisfied, different tunneling models yield only slightly different precise values of $J_{c,d}^J(\phi_0)$ for $0 < \phi_0 < \pi/4$.

To the extent that Bi2212 is slightly orthorhombic, a bit of a $g_{xy(x^2-y^2)}$ -wave OP component can mix with a

$d_{x^2-y^2}$ -wave OP, in which the mixing would shift the angle at which $J_{c,d}^J(\phi_0) = 0$ slightly away from $\pi/4$.⁴⁰ In addition, if there is a secondary phase transition, such as one that mixes OP's of $d_{x^2-y^2}$ - and either d_{xy} - or s -wave symmetry, then this theorem does not apply.⁴⁰ However, we showed that for parameters relevant to Bi2212, such a possibility could only hope to explain low- T data, not the data near T_c .⁴⁰ In addition, higher-order tunneling processes were shown to give a finite but entirely negligible contribution to $J_{c,d}^J(\pi/4)$.⁴¹ We remark that there have been a number of theories of the HTSC that relied upon coherent tunneling in the c axis, with a \mathbf{k} -dependent matrix element, between each of the layers.^{46,47} But, that model not only gives $J_{c,d}^J(\pi/4) = 0$, it gave the worst agreement with the experiment of Li *et al.* of all of the coherent tunneling models studied, even for an ordinary s -wave OP.⁴¹

The theorem holds for an arbitrary $f^J(\mathbf{k}, \mathbf{k}')$ and for an arbitrary form of a d -wave OP. But we would like to determine quantitatively the dependencies of the $J_{c,s}^J(\phi_0, T)$ and $J_{c,d}^J(\phi_0, T)$, both for a variety of tunneling models and for a variety of s and $d_{x^2-y^2}$ OP forms. In particular, when the tunneling is not purely incoherent, differences could arise.

In order to investigate how sensitive our results are to the particular form of the OP, and still be consistent with the c -axis twist experiments, we have made a systematic study of the effect of various OP anisotropies, using the weak-coupling BCS theory of superconductivity. In this study, we did not vary the pairing interaction directly, but only assumed that the OP had a variety of particular forms that differed sufficiently from each other, in order to be as general in our conclusions as possible. We study the gap functions $\psi_{i\zeta\epsilon}(\mathbf{k})$ corresponding to the OP's $\Delta_{i\zeta\epsilon}(\mathbf{k}, T) = \Delta_0(T) \psi_{i\zeta\epsilon}(\mathbf{k})$ for general s - and $d_{x^2-y^2}$ -wave superconductors with $\zeta = s, d$, and $i = o, e, c, a$, respectively,

$$\psi_{os}(\mathbf{k}) = 1, \quad (8)$$

$$\psi_{es\epsilon}(\mathbf{k}) = \{[\cos(k_x a) - \cos(k_y a)]^2 + \epsilon^2\}^{1/2} / (1 + \epsilon^2)^{1/2}, \quad (9)$$

$$\psi_{cs\epsilon}(\mathbf{k}) = [\sin^2(k_x a) \sin^2(k_y a) + \epsilon^2]^{1/2} / (1 + \epsilon^2)^{1/2}, \quad (10)$$

$$\psi_{as}(\mathbf{k}) = \cos(k_x a) + \cos(k_y a), \quad (11)$$

$$\psi_{od}(\mathbf{k}) = \cos(k_x a) - \cos(k_y a), \quad (12)$$

$$\psi_{ed\epsilon}(\mathbf{k}) = [\cos(k_x a) - \cos(k_y a)] \{[\cos(k_x a) - \cos(k_y a)]^2 + \epsilon^2\}^{1/2} / (1 + \epsilon^2)^{1/2}, \quad (13)$$

$$\psi_{cd\epsilon}(\mathbf{k}) = [\cos(k_x a) - \cos(k_y a)] [\sin^2(k_x a) \sin^2(k_y a) + \epsilon^2]^{1/2} / (1 + \epsilon^2)^{1/2}, \quad (14)$$

and

$$\psi_{ad}(\mathbf{k}) = [\cos(k_x a) - \cos(k_y a)] [\cos(k_x a) + \cos(k_y a)]. \quad (15)$$

For simplicity, we shall denote these the ‘‘ordinary- s -wave,’’ ‘‘extended- s -wave,’’ ‘‘compressed- s -wave,’’ ‘‘anomalous-

s -wave,” “ordinary- $d_{x^2-y^2}$ -wave,” “extended- $d_{x^2-y^2}$ -wave,” “compressed- $d_{x^2-y^2}$ -wave,” and “anomalous- $d_{x^2-y^2}$ -wave” OP’s, respectively.⁴⁸ Since the ordinary- and anomalous- s - and $d_{x^2-y^2}$ -wave OP’s do not depend upon the parameter ϵ , we drop the ϵ in their gap function subscripts.

Setting $\epsilon \rightarrow 0$ leads to the “fully extended-” or “fully compressed-” s -wave and $d_{x^2-y^2}$ -wave forms, each proportional to $|\cos(k_x a) - \cos(k_y a)|$ and $|\sin(k_x a)\sin(k_y a)|$, respectively, which have nodes at the same places on the Fermi surface as do the ordinary- $d_{x^2-y^2}$ - and d_{xy} -wave superconductors, respectively. The first four and the second four are specific examples of the “general- s -wave” and “general- $d_{x^2-y^2}$ -wave” OP’s,

$$\psi_{is\epsilon}(\mathbf{k}) = \sum_{n,m=0}^{\infty} a_{i,nm}(\epsilon) \cos(nk_x a) \cos(mk_y a) \quad (16)$$

and

$$\begin{aligned} \psi_{id\epsilon}(\mathbf{k}) = & \sum_{n,m=0}^{\infty} \tilde{a}_{i,nm}(\epsilon) [\cos(k_x a) - \cos(k_y a)] \\ & \times \cos(nk_x a) \cos(mk_y a), \end{aligned} \quad (17)$$

respectively, where $a_{i,nm}(\epsilon) = a_{i,mn}(\epsilon)$ and $\tilde{a}_{i,nm}(\epsilon) = \tilde{a}_{i,mn}(\epsilon)$, which were described previously.⁴⁰ Here we take $\tilde{a}_{i,nm}(\epsilon) = a_{i,nm}(\epsilon)$.

We remark that the anomalous- s -wave OP changes sign on the tight-binding Fermi surface, and averages to zero over the first BZ. However, its average on the tight-binding Fermi surface is not zero, so we include it for comparison. The simplest coefficients are for the ordinary and anomalous functions, which are

$$a_{o,nm} = \delta_{n,0} \delta_{m,0} \quad (18)$$

and

$$a_{a,nm} = \delta_{n,1} \delta_{m,0} + \delta_{n,0} \delta_{m,1},$$

respectively, where $\delta_{n,0}$ is the Kronecker delta. The full set of coefficients $a_{i,nm}(0)$ for $i=c,e$ from which the $\psi_{i\zeta 0}(\mathbf{k})$ are constructed are given in Appendix A. Keeping only the leading terms in the expansions for $\psi_{es0}(\mathbf{k})$ and $\psi_{cs0}(\mathbf{k})$ in the $\epsilon \rightarrow 0$ limit, one finds

$$\begin{aligned} \psi_{es0}(\mathbf{k}) \rightarrow & \frac{8}{\pi^2} \left(1 - \frac{4}{3} \cos(k_x a) \cos(k_y a) \right. \\ & \left. + \frac{2}{9} [\cos(2k_x a) + \cos(2k_y a)] + \dots \right) \end{aligned} \quad (19)$$

and

$$\psi_{cs0}(\mathbf{k}) \rightarrow \frac{4}{\pi^2} \left(1 - \frac{2}{3} [\cos(2k_x a) + \cos(2k_y a)] + \dots \right). \quad (20)$$

When the phenomenological pairing interaction $\lambda \psi_{es0}(\mathbf{k}) \psi_{es0}(\mathbf{k}')$, which leads to the gap function $\psi_{es0}(\mathbf{k})$, is transformed into real space, one sees that $\psi_{es0}(\mathbf{k})$ involves

strong on-site pairing, stronger next-nearest neighbor repulsion, weak next-next-nearest-neighbor attraction, and the remaining real-space interaction terms are successively weaker. Similarly, $\psi_{cs0}(\mathbf{k})$ involves strong on-site pairing, slightly weaker next-next-nearest-neighbor repulsion, etc. Setting $\epsilon \neq 0$ modifies the relative strengths of the $a_{e,nm}(\epsilon)$ and $a_{c,nm}(\epsilon)$.

We also studied the $d_{x^2-y^2}$ -wave OP obtained from the repulsive interaction,^{49,50}

$$V(\mathbf{q}) = -V_0 \sum_{\mathbf{Q}=(\pm 1, \pm 1)\pi/a} \Gamma / [(\mathbf{q} - \mathbf{Q})^2 + \Gamma^2], \quad (21)$$

where $V_0 = 556$ meV and $\Gamma = 0.1$. The BCS equation was solved for $\Delta(\mathbf{k}, T)$ in terms of $V(\mathbf{k} - \mathbf{k}')$, yielding $\Delta(\mathbf{k}, T) = \Delta_0(T) \varphi_d(\mathbf{k})$. We then constructed an extended- s -wave OP from the absolute magnitude of the $d_{x^2-y^2}$ -wave form obtained from Eq. (21), $\varphi_{es}(\mathbf{k}) = |\varphi_d(\mathbf{k})|$. The isotropic s -wave OP was taken to have its maximum magnitude, $\varphi_s(\mathbf{k}) = \max_{\mathbf{k}} \{|\varphi_d(\mathbf{k})|\}$, a constant. The main differences between these models and the OP forms studied in Eqs. (8)–(15) are that the d -wave and extended- s -wave forms so obtained have somewhat different wave-vector forms from those with $\epsilon = 0$ in Eqs. (12) and (9), respectively. We included the umklapp terms which occur with rotated Fermi surfaces, but the effects of doing so were very small in all cases we studied, as found previously.⁴¹

We remark that this particular form of pairing interaction does not easily lead to an extended- s -wave form of the OP, even when one changes the sign of the interaction, or adds an attractive term of similar form. However, semimicroscopic models of the pairing interaction exist which result in highly anisotropic OP’s of general- s -wave symmetry,⁵¹ some of which even give OP’s with nodes.⁵² One such model is based upon the work of Andersen *et al.*,⁴⁶ in which they showed that the interaction could be large only at rather isolated points in the BZ. Although those authors did not explicitly consider an s -wave state, we have modified their procedures to do so. Through the various hopping matrix elements, the interaction between the quasiparticles depends upon their particular positions within the BZ. This is particularly true when one considers the large density of states present on the saddle bands, such as those near to the \bar{M} point in the first BZ of Bi2212. Such an interaction could give an OP that is nearly zero over large regions of the BZ, and hence over finite regions of the Fermi surface. In general, an extended- s -wave gap function proportional to $\varphi_{es}(\mathbf{k})$ is consistent with essentially all non-phase-sensitive experiments.

We shall also use a simpler model, which might be appropriate for electron-doped HTSC, with an isotropic in-plane quasiparticle dispersion. Assuming as usual that the main contributions to all the momentum integrals come from the vicinity of the Fermi surface, we can integrate out the quasiparticle energy. We then only need to consider the OP’s on a circular Fermi surface, which allows us to perform many of the calculations analytically.

In analogy with the real-space pairing OP’s, we study the Fermi-surface-restricted pairing ordinary-, extended-,

compressed-, and anomalous- s - and $d_{x^2-y^2}$ -wave OP's, respectively, $\Delta_{i\zeta\epsilon}(\phi_{\mathbf{k}}, T) = \Delta_0(T) \tilde{\psi}_{i\zeta\epsilon}(\phi_{\mathbf{k}})$, where $i = o, e, c, a$, and $\zeta = s, d$,

$$\tilde{\psi}_{os}(\phi_{\mathbf{k}}) = 1, \quad (22)$$

$$\tilde{\psi}_{es\epsilon}(\phi_{\mathbf{k}}) = [\cos^2(2\phi_{\mathbf{k}}) + \epsilon^2]^{1/2}/(1 + \epsilon^2)^{1/2}, \quad (23)$$

$$\tilde{\psi}_{cs\epsilon}(\phi_{\mathbf{k}}) = [\sin^2(2\phi_{\mathbf{k}}) + \epsilon^2]^{1/2}/(1 + \epsilon^2)^{1/2}, \quad (24)$$

$$\tilde{\psi}_{as\epsilon}(\phi_{\mathbf{k}}) = [\epsilon + \cos(4\phi_{\mathbf{k}})]/(1 + |\epsilon|), \quad (25)$$

$$\tilde{\psi}_{od}(\phi_{\mathbf{k}}) = \cos(2\phi_{\mathbf{k}}), \quad (26)$$

$$\tilde{\psi}_{ed\epsilon}(\phi_{\mathbf{k}}) = \cos(2\phi_{\mathbf{k}})[\cos^2(2\phi_{\mathbf{k}}) + \epsilon^2]^{1/2}/(1 + \epsilon^2)^{1/2}, \quad (27)$$

$$\tilde{\psi}_{cd\epsilon}(\phi_{\mathbf{k}}) = \cos(2\phi_{\mathbf{k}})[\sin^2(2\phi_{\mathbf{k}}) + \epsilon^2]^{1/2}/(1 + \epsilon^2)^{1/2}, \quad (28)$$

and

$$\tilde{\psi}_{ad\epsilon}(\phi_{\mathbf{k}}) = \cos(2\phi_{\mathbf{k}})[\epsilon + \cos(4\phi_{\mathbf{k}})]/(1 + |\epsilon|), \quad (29)$$

respectively. We allow the anomalous OP's to have an $\epsilon \neq 0$ in order that the average over the Fermi surface of $\tilde{\psi}_{as\epsilon}(\phi_{\mathbf{k}})$ might be finite. These and similar functions may be written as Fourier series, in analogy to Eqs. (16) and (17),

$$\tilde{\psi}_{is\epsilon}(\phi_{\mathbf{k}}) = \sum_{n=0}^{\infty} a_{isn}(\epsilon) \cos(4n\phi_{\mathbf{k}}) \quad (30)$$

and

$$\tilde{\psi}_{id\epsilon}(\phi_{\mathbf{k}}) = \sum_{n=0}^{\infty} a_{idn}(\epsilon) \cos[(4n+2)\phi_{\mathbf{k}}], \quad (31)$$

for $i = o, e, c, a$, respectively. The ordinary and anomalous coefficients are

$$a_{osn} = a_{odn} = \delta_{n,0}, \quad (32)$$

$$a_{asn}(\epsilon) = \frac{\epsilon \delta_{n,0} + \delta_{n,1}}{1 + |\epsilon|}, \quad (33)$$

and

$$a_{adn}(\epsilon) = \frac{(2\epsilon + 1)\delta_{n,0} + \delta_{n,1}}{2(1 + |\epsilon|)}.$$

The extended and compressed coefficients $a_{i\zeta n}(0)$ for $i = e, c$ and $\zeta = s, d$ are given in Appendix A.

III. THE TUNNELING MODELS

We shall assume that $f^J(\mathbf{k}, \mathbf{k}') = f^J(\mathbf{k} - \mathbf{k}')$ satisfies time-reversal invariance and depends only upon the change in the quasiparticle momentum parallel to the tunnel junction, $\mathbf{k} - \mathbf{k}'$. Previously, we investigated the case in which $f^J(\mathbf{k} - \mathbf{k}') \propto \delta(\mathbf{k} - \mathbf{k}')$, appropriate for coherent tunneling.⁴¹ We found that it made very little difference whether or not one

included umklapp terms in the integrals in Eq. (1). We solved the model to all orders in the tunneling strength, optimizing $J_c^J(\phi_0)$ with respect to the phase difference across adjacent junctions. For the ordinary- $d_{x^2-y^2}$ -wave OP, weak coherent tunneling always gave $J_{c,d}^J(\pi/4) = 0$. Although higher-order coherent tunneling processes allowed $J_{c,d}^J(\pi/4) \neq 0$, inevitably $J_{c,d}^J(\pi/4)/J_{c,d}^J(0) \ll 1$ for all $T \leq T_c$,⁴¹ so that it was still impossible to fit the data of Li *et al.* with a d -wave OP. Twisting of the nominally $d_{x^2-y^2}$ -wave OP by mixing in components of d_{xy} symmetry was found to give a potentially substantial $J_{c,d}^J(\pi/4)/J_{c,d}^J(0)$ for $T \leq T_c$, but we always found $J_{c,d}^J(\pi/4)/J_{c,d}^J(0) \ll 1$ near T_c .⁴⁰ For Bi2212, the c -axis tunneling is so much weaker than the in-plane intersite hopping strength, that $J_{c,d}^J(\pi/4)/J_{c,d}^J(0) \ll 1$ for a wide- T region below T_c .

However, we found that for Fermi surfaces similar to that pictured in Fig. 1, even for an isotropic s -wave OP, it was not possible to obtain a quantitative fit to the data with coherent tunneling.^{8,41} We then argued that for extremely incoherent tunneling, with $f^J(\mathbf{k} - \mathbf{k}') = f_0^J$, a constant, the s -wave and extended- s -wave OP's could both fit the data quantitatively. But, we did not discuss the intermediate tunneling coherence cases in any detail, and that is our purpose here. To be as general as possible, we shall study five tunneling models which interpolate between these two limits, using the eight OP's of s - and $d_{x^2-y^2}$ -wave symmetry described in Eqs. (8)–(15).

The most natural model quantifying the coherence of the tunneling matrix element squared is a Gaussian function of $\mathbf{k} - \mathbf{k}'$,

$$f_G^J(\mathbf{k} - \mathbf{k}') = f_{0G}^J \exp[-(\mathbf{k} - \mathbf{k}')^2/\tilde{\sigma}^2], \quad (34)$$

where

$$\tilde{\sigma} = 2^{1/2} \pi \sigma / a. \quad (35)$$

Since $\sigma = 0$ and $\sigma \rightarrow \infty$ result in purely coherent and incoherent tunneling, σ is the dimensionless parameter quantifying the coherence of the tunneling. In addition, we shall study four other models,

$$f_E^J(\mathbf{k} - \mathbf{k}') = f_{0E}^J \exp[-|\mathbf{k} - \mathbf{k}'|/\tilde{\sigma}], \quad (36)$$

$$f_L^J(\mathbf{k} - \mathbf{k}') = \frac{f_{0L}^J}{[1 + (k_x - k'_x)^2/\tilde{\sigma}^2][1 + (k_y - k'_y)^2/\tilde{\sigma}^2]}, \quad (37)$$

$$f_{RL}^J(\mathbf{k} - \mathbf{k}') = \frac{f_{0RL}^J}{1 + (\mathbf{k} - \mathbf{k}')^4/\tilde{\sigma}^4}, \quad (38)$$

and

$$f_{SL}^J(\mathbf{k} - \mathbf{k}') = \frac{f_{0SL}^J}{1 + (\mathbf{k} - \mathbf{k}')^2/\tilde{\sigma}^2}, \quad (39)$$

which are exponential, Lorentzian, rotationally invariant Lorentzian, and ‘‘stretched Lorentzian,’’ respectively, in $\mathbf{k} - \mathbf{k}'$. We included the exponential and Lorentzian models, which are nonanalytic in $\mathbf{k} - \mathbf{k}'$ and nonrotationally invari-

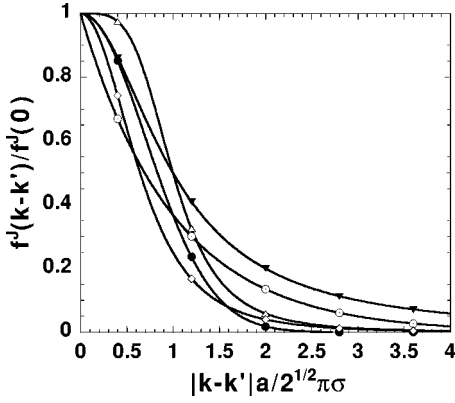


FIG. 2. Plots of $f^J(\mathbf{k}-\mathbf{k}')$ for the five models of the tunneling matrix element squared. The Gaussian (solid circles), exponential (open circles), rotationally invariant Lorentzian (open triangles), and stretched Lorentzian (solid inverted triangles) models are shown as indicated. f^J for the Lorentzian model varies from the curve with open diamonds for $|k_x-k'_x|=|k_y-k'_y|$ to that of the stretched Lorentzian (solid inverted triangles) for either $k_x=k'_x$ or $k_y=k'_y$.

ant, respectively, in order to investigate the most general types of tunneling behavior that can occur between the coherent and incoherent limits. In addition, we included both the rotationally invariant and stretched Lorentzian models, since their leading contributions near the incoherent limit coupling d -wave superconductors have different signs. The f_{0i}^J are constants that normalize the overall tunneling to a particular strength, which we characterize equivalently for $i = G, E, L, RL, SL$ in terms of an effective c -axis “scattering rate” $1/\tau_\perp$ for all processes in the first BZ,⁵³

$$\langle f_i^J(\mathbf{k}-\mathbf{k}') \rangle = 1/\tau_\perp. \quad (40)$$

Similar models were employed by others.^{25,53–56} In Fig. 1, the shaded concentric circles indicate how the range of momentum states accessible by tunneling from the central point increases with σ^2 . In the shaded regions, $1/e \leq f_G^J(\mathbf{k}-\mathbf{k}')/f_{0G}^J, f_E^J(\mathbf{k}-\mathbf{k}')/f_{0E}^J \leq 1$ and $1/2 \leq f_{RL}^J(\mathbf{k}-\mathbf{k}')/f_{0L}^J, f_{SL}^J(\mathbf{k}-\mathbf{k}')/f_{0SL}^J \leq 1$. For a given σ^2 , the various models differ considerably, when one defines a range of tunneling processes by requiring f^J to be less than some fraction of its maximum. We note that for the Lorentzian model, one would have to replace these concentric circles with concentric figures of tetragonal symmetry, having minima along the x and y axes, and maxima along the diagonals. The dependence of each of these tunneling functions upon $|\mathbf{k}-\mathbf{k}'|$ is shown in Fig. 2. For the Lorentzian model, we only showed the dependencies along the axes and the diagonals.

A. Circular Fermi-surface models

For a circular Fermi-surface cross section, we write $\mathbf{k} = k_F(\cos \phi_k, \sin \phi_k)$, etc. Then, Eqs. (34)–(39) can be rewritten, letting

$$\gamma = (ak_F/\pi\sigma)^2, \quad (41)$$

leading to

$$f_G^J(\phi_k - \phi_{k'}) = \tilde{f}_{0G}^J \exp\{-\gamma[1 - \cos(\phi_k - \phi_{k'})]\}, \quad (42)$$

$$f_E^J(\phi_k - \phi_{k'}) = \tilde{f}_{0E}^J \exp\{-\sqrt{2\gamma}|\sin[(\phi_k - \phi_{k'})/2]|\}, \quad (43)$$

$$f_L^J(\phi_k, \phi_{k'}) = \frac{\tilde{f}_{0L}^J}{[1 + \gamma(\cos \phi_k - \cos \phi_{k'})^2][1 + \gamma(\sin \phi_k - \sin \phi_{k'})^2]}, \quad (44)$$

$$f_{RL}^J(\phi_k - \phi_{k'}) = \frac{\tilde{f}_{0RL}^J}{1 + \gamma^2[1 - \cos(\phi_k - \phi_{k'})]^2}, \quad (45)$$

and

$$f_{SL}^J(\phi_k - \phi_{k'}) = \frac{\tilde{f}_{0SL}^J}{1 + \gamma[1 - \cos(\phi_k - \phi_{k'})]}, \quad (46)$$

where the \tilde{f}_{0i}^J are different normalization constants. The Gaussian function, $f_G^J(\phi_k - \phi_{k'})$, is identical to that of Graf *et al.*,⁵³ provided that $\tilde{f}_{0G}^J = \exp(\gamma)/[\tau_\perp I_0(\gamma)]$, where $I_n(z)$ is a Bessel function and $1/\tau_\perp$ is the effective interlayer tunneling rate,

$$1/\tau_\perp = \int_0^{2\pi} d\phi f_i^J(\phi)/2\pi \quad (48)$$

and

$$1/\tau_\perp = \int_0^{2\pi} d\phi \int_0^{2\pi} d\phi' f_L^J(\phi, \phi')/(2\pi)^2 \quad (49)$$

for the rotationally invariant models and for the Lorentzian model, respectively.

We first consider an *arbitrary* rotationally invariant $f^J(\gamma, \phi_k - \phi_{k'})$ on a circular Fermi-surface cross section, where γ is the parameter characterizing f^J such that in the incoherent limit, $\gamma \rightarrow 0$, $f^J(0, \phi_k - \phi_{k'}) = 1/\tau_\perp$, and in the coherent limit, $\gamma \rightarrow \infty$, $f^J(\infty, \phi_k - \phi_{k'}) = \delta(\phi_k - \phi_{k'})/\tau_\perp$, respectively. To do so, we write f^J in terms of its Fourier series.

$$f^J(\gamma, \phi_k - \phi_{k'}) = \frac{1}{\tau_\perp} \sum_{n=0}^{\infty} f_n(\gamma) \cos[n(\phi_k - \phi_{k'})], \quad (50)$$

where

$$f_n(\gamma) = \frac{\int_0^{2\pi} d\phi f^J(\gamma, \phi) \cos(n\phi)}{\int_0^{2\pi} f^J(\gamma, \phi) d\phi}. \quad (51)$$

For the Lorentzian model, $f_L^J(\gamma, \phi_k, \phi_{k'})$ may be expanded as

$$f_L^J(\gamma, \phi_k, \phi_{k'}) = \frac{1}{\tau_\perp} \sum_{n,m=0}^{\infty} f_{n,m}^L(\gamma) \cos[2n(\phi_k - \phi_{k'})] \times \cos[4m(\phi_k + \phi_{k'})]. \quad (52)$$

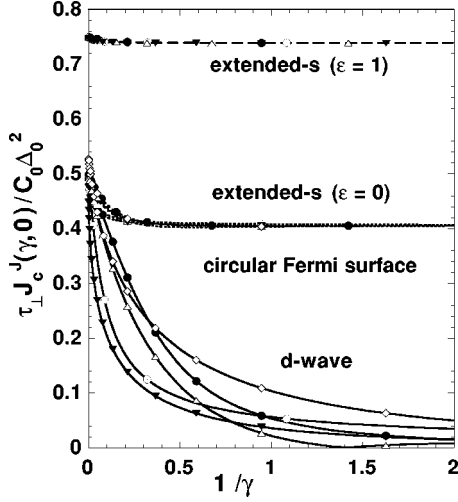


FIG. 3. Plots of $\tau_{\perp} J_c^J / C_0 \Delta_0^2$ at T_c and $\phi_0 = 0$, which is $f_{ie\epsilon}(\gamma, 0)$ and $f_{od}(\gamma)$ for the extended- and compressed- s -wave with $\epsilon = 0$ (dotted curves) and $\epsilon = 1$ (dashed curves), and ordinary- $d_{x^2-y^2}$ -wave (solid curves) OP's on the circular Fermi surface, respectively, versus $1/\gamma$. Results for the Gaussian (solid circles), exponential (open circles), rotationally invariant Lorentzian (open triangles), stretched Lorentzian (solid inverted triangles), and Lorentzian (open diamonds) models are shown.

The $f_n(\gamma)$ for the four specific rotationally invariant models and the $f_{n,m}^L(\gamma)$ are given in Appendix B, along with some useful asymptotic expansions near the coherent and incoherent limits.

Just below T_c , $\Delta_0(T) \rightarrow 0$, and

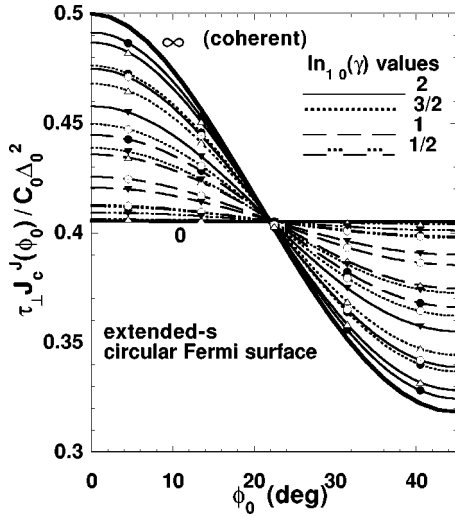


FIG. 4. Plots of $f_{is0}(\gamma, \phi_0) = \tau_{\perp} J_{c, is0}^J(\phi_0) / C_0 \Delta_0^2$ just below T_c for the extended- and compressed- s -wave OP's ($i = e, c$) on a circular Fermi surface, as a function of ϕ_0 , at the γ values 10^x , where $x = 0$ (thick line), $1/2$ (dash-dotted), 1 (dashed), $3/2$ (dotted), 2 (thin solid), and for the coherent limit $\gamma \rightarrow \infty$ (thick solid curve). Results for the Gaussian (solid circles), exponential (open circles), rotationally invariant Lorentzian (open triangles), stretched Lorentzian (inverted solid triangles), and Lorentzian (open diamonds) models are shown.

$$J_{c, i\zeta\epsilon}^J(\gamma, \phi_0) = C_0 |\langle f^J(\gamma, \phi_{\mathbf{k}}, \phi_{\mathbf{k}'}) \Delta_{i\zeta\epsilon}(\phi_{\mathbf{k}}, T) \Delta_{i\zeta\epsilon}(\phi_{\mathbf{k}'}, T) \rangle_{\phi_{\mathbf{k}}, \phi_{\mathbf{k}'}}|, \quad (53)$$

where $C_0 = em^2 / (4T_c)$, m is the in-plane effective mass, $\zeta = s, d$ and $i = o, e, c, a$ index the OP's, and $\phi_{\mathbf{k}'} = \phi_{\mathbf{k}} + \phi_0$. We find for a general rotationally invariant tunneling model that

$$J_{c, i\zeta\epsilon}^J(\gamma, \phi_0) = C_0 \Delta_0^2(T) |f_{i\zeta\epsilon}(\gamma, \phi_0)| / \tau_{\perp}, \quad (54)$$

for $i = o, e, c, a$ and $\zeta = s, d$, where

$$f_{is\epsilon}(\gamma, \phi_0) = \frac{1}{2} \sum_{n=0}^{\infty} (1 + \delta_{n,0}) a_{isn}^2(\epsilon) \cos(4n\phi_0) f_{4n}(\gamma), \quad (55)$$

$$f_{id\epsilon}(\gamma, \phi_0) = \frac{1}{2} \sum_{n=0}^{\infty} a_{idn}^2(\epsilon) \cos[(4n+2)\phi_0] f_{4n+2}(\gamma), \quad (56)$$

and the $f_n(\gamma)$ are given by Eq. (51). These results are presented in Figs. 3–6.

For the Lorentzian model, Eq. (54) still applies, but the functions $f_{is\epsilon}(\gamma, \phi_0)$ and $f_{id\epsilon}(\gamma, \phi_0)$ for $i = o, e, c, a$ are, respectively replaced by

$$f_{is\epsilon}(\gamma, \phi_0) = \frac{1}{2} \sum_{n,m=0}^{\infty} a_{isn}(\epsilon) a_{ism}(\epsilon) \cos(4m\phi_0) \times [f_{2(n+m), |n-m|}^L(\gamma) + f_{2|n-m|, n+m}^L(\gamma)] \quad (57)$$

and

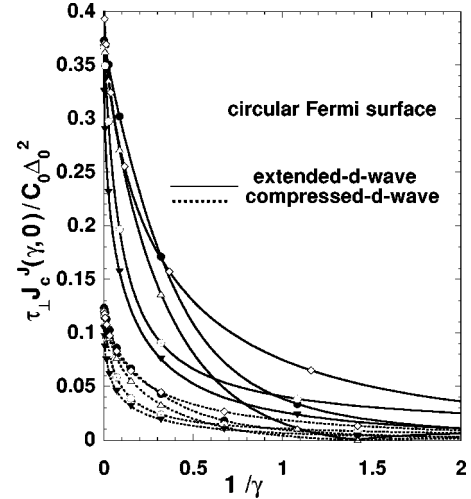


FIG. 5. Plots of $f_{id0}(\gamma, 0) = \tau_{\perp} J_c^J / C_0 \Delta_0^2$ at T_c , $\epsilon = 0$, and $\phi_0 = 0$, for the extended- (dotted) and compressed- (solid) $d_{x^2-y^2}$ -wave OP's on the circular Fermi surface, respectively, versus $1/\gamma$. Results for the Gaussian (solid circles), exponential (open circles), rotationally invariant Lorentzian (open triangles), stretched Lorentzian (inverted solid triangles), and Lorentzian (open diamonds) models are shown.

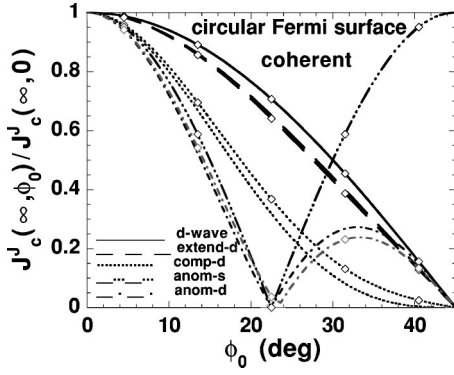


FIG. 6. Plots of $J_c^J(\phi_0)/J_c^J(0)$ at T_c and the coherent limit $\gamma \rightarrow \infty$, for the ordinary- $d_{x^2-y^2}$ -wave (solid), $|\cos(2\phi_0)|$, extended- $d_{x^2-y^2}$ -wave (dashed), compressed- $d_{x^2-y^2}$ -wave (dotted), and anomalous- $d_{x^2-y^2}$ -wave (dash-dotted) $f_{id0}(\infty, \phi_0)$ ($\epsilon=0$), and the anomalous- s -wave (dash-dot-dot-dotted) $f_{as0}(\infty, \phi_0)$ on a circular Fermi surface, respectively, with rotationally invariant tunneling matrix elements squared. Results for the Lorentzian (open diamonds) model are also shown.

$$f_{id\epsilon}(\gamma, \phi_0) = \frac{1}{2} \sum_{n,m=0}^{\infty} a_{idn}(\epsilon) a_{idm}(\epsilon) \cos[(4m+2)\phi_0] \times [f_{2|n-m|,n+m+1}^L(\gamma) + f_{2(n+m+1),|n-m|}^L(\gamma)]. \quad (58)$$

The ordinary- $d_{x^2-y^2}$ -wave $J_{c,od}^J(\gamma, \phi_0) \propto |f_{od}(\gamma, \phi_0)|$. In the four rotationally invariant models, $f_{od}(\gamma, \phi_0) = \cos(2\phi_0)f_2(\gamma)/2$, and in the Lorentzian model, $f_{od}(\gamma, \phi_0) = \cos(2\phi_0)[f_{2,0}^L(\gamma) + f_{0,1}^L(\gamma)]/2$. Hence, we conclude that for all five tunneling models, $J_{c,od}^J(\gamma, \phi_0) \propto |\cos(2\phi_0)|$, even for the Lorentzian model, which is somewhat surprising, as it is not rotationally invariant. We note that these calculations were only performed just below T_c , and one might therefore imagine that a more complicated ϕ_0 dependence would occur at lower T . As shown in the following, however, such corrections are weak, and do not change the result of the theorem that $J_{c,d}(\gamma, \pi/4) = 0$ for all $T \leq T_c$. In addition, in the incoherent limit, $f_{od}(0, \phi_0) = 0$, with the exponential model giving the slowest approach to 0. In contrast, the ordinary- s -wave $J_{c,os}^J(\gamma, \phi_0) \propto |f_{os}(\gamma, \phi_0)| = 1$ for all five tunneling models is completely independent of ϕ_0 and of the details of $f^J(\gamma, \phi_{\mathbf{k}}, \phi_{\mathbf{k}'}) \forall \gamma$.

At $\phi_0 = 0$, the ordinary- $d_{x^2-y^2}$ -wave functions $f_{od}(\gamma, 0)$ for all five tunneling models are plotted versus $1/\gamma$ in Fig. 3. The rotationally invariant Lorentzian model gives rise to a $f_{od}(\gamma, 0)$ that changes sign with decreasing γ , as evidenced by comparing Eqs. (B7) and (B11) and by examining the figure. This is not too surprising, because in the approach to the incoherent limit, the tunneling process can occur between different lobes of the $d_{x^2-y^2}$ -wave OP, which can give a negative contribution to $J_{c,ide}^J(\gamma, 0)$. Whether an overall positive or negative sign wins thus depends on the precise details of the falloff of $f^J(\phi_{\mathbf{k}} - \phi_{\mathbf{k}'})$ with $\phi_{\mathbf{k}} - \phi_{\mathbf{k}'}$. Almost all models, including the four other models we have explicitly studied, give rise to a positive overall value, but the rotation-

ally invariant Lorentzian model is special, since expanding Eq. (45) to order γ^2 leads to a negative leading term for $J_{c,ide}^J(\gamma, 0)$ for sufficiently small γ . In addition, it is easily seen from Fig. 3 that the Lorentzian model gives the largest ordinary- $d_{x^2-y^2}$ -wave $f_{od}(\gamma, 0)$ value at intermediate γ values in this circular Fermi-surface calculation. For smaller γ values (not pictured), the exponential model gives the largest $f_{od}(\gamma, 0)$. The same qualitative features are seen for the extended- d -wave and compressed- d -wave models, as shown in Fig. 5. Regardless of the value of γ [e.g., even when γ is near to the value at which $f_{id\epsilon}(\gamma, 0)$ changes sign in the rotationally invariant tunneling model], Eq. (56) shows that $f_{id\epsilon}(\gamma, \phi_0)$ has the same basic ϕ_0 dependence as for any other γ value, vanishing at $\phi_0 = 0$.

For the general Fermi-surface restricted model, $J_{c,ise}^J(\gamma, \phi_0)/J_{c,s}^J = f_{ise}(\gamma, \phi_0)$ at T_c , which is periodic in ϕ_0 with period $\pi/2$, satisfying $f_{ise}(\gamma, \pm\pi/2 - \phi_0) = f_{ise}(\gamma, \phi_0)$ for $i=c, e, a$. We first consider the anomalous- s -wave case, $f_{ase}(\gamma, \phi_0) = [\epsilon^2 + \frac{1}{2}f_4(\gamma)\cos(4\phi_0)]/(1+|\epsilon|)^2$. For each rotationally invariant tunneling model, this varies smoothly between the coherent limit $[\epsilon^2 + \frac{1}{2}\cos(4\phi_0)]/(1+|\epsilon|)^2$ and the incoherent limit $\epsilon^2/(1+|\epsilon|)^2$. For the Lorentzian model, $f_{ase}(\gamma, \phi_0) = \{\epsilon^2 + \epsilon[1 + \cos(4\phi_0)]f_{2,1}^L(\gamma) + \frac{1}{2}\cos(4\phi_0)[f_{0,2}^L(\gamma) + f_{4,0}^L(\gamma)]\}/(1+|\epsilon|)^2$. This has the same incoherent limit as for the rotationally invariant tunneling models, but the coherent limit also contains a ϕ_0 -independent part that vanishes in the incoherent limit. We note that the “fully” anomalous- s -wave OP has $f_{as0}(\gamma, \phi_0) \propto \cos(4\phi_0)$, with a coefficient, $f_4(\gamma)/2$ or $[f_{0,2}^L(\gamma) + f_{4,0}^L(\gamma)]/2$ for the Lorentzian model, that vanishes in the incoherent limit. $J_{c,as0}^J(\gamma, \phi_0)$ vanishes at $\phi_0 = \pi/8$, but not at $\pi/4$, as shown in Fig. 6.

Next, we consider the $i=e, c$ s -wave cases. For the four rotationally invariant models, these functions are identical. In Fig. 3, we show the very weak γ dependence of $f_{ie\epsilon}(\gamma, 0)$ for $\epsilon=0, 1$ for all five tunneling models. In Fig. 4, we plot $f_{ie0}(\gamma, \phi_0)$ for the four rotationally invariant models. We omitted the Lorentzian model for clarity of presentation. In the coherent limit for $\epsilon=0$, $f_{is0}(\infty, \phi_0) = [|\sin(2\phi_0)| + (\pi/2 - 2|\phi_0|)\cos(2\phi_0)]/\pi$ in the domain $|\phi_0| \leq \pi/2$. $f_{is0}(\infty, \phi_0)$ has maxima of $1/2$ at $\phi_0 = n\pi/2$ and minima of $1/\pi$ at $\phi_0 = (2n+1)\pi/4$ for integer n . In the incoherent limit $\gamma \rightarrow 0$ for all five tunneling models, $f_{is\epsilon}(0, \phi_0) \rightarrow [2E(k)/\pi]^2$, where $k = (\epsilon^2 + 1)^{-1/2}$ and $E(k)$ is a complete elliptic integral. In addition, regardless of γ and of the form of $f^J(\gamma, \phi_{\mathbf{k}} - \phi_{\mathbf{k}'})$, the mean value $(4/\pi) \int_0^{\pi/4} d\phi_0 f_{is\epsilon}(\gamma, \phi_0) = [2E(k)/\pi]^2$, precisely the incoherent limit. This reduces to $(2/\pi)^2$ and 1 in the $\epsilon \rightarrow 0$ and $\epsilon \rightarrow \infty$ limits, respectively.

In addition, the s -wave functions $f_{is\epsilon}(\gamma, 0)$ for $i=c, e$ also decrease from $(1/2 + \epsilon^2)/(1 + \epsilon^2)$ at $\gamma \rightarrow \infty$ with decreasing γ , but not nearly as dramatically, approaching $[2E(k)/\pi]^2$ as $\gamma \rightarrow 0$, nearly independent of the details of the tunneling model. For small ϵ , however, $f_{ase}(\gamma, 0)$ decreases dramatically, almost as much as $f_{od}(\gamma, 0)$, as the $\cos(4\phi_0)$ part of $f_{ase}(\gamma, \phi_0)$ gets washed out by the rapidly decreasing $f_4(\gamma)$ coefficient. In the isotropic s -wave limit $\epsilon \rightarrow \infty$, $f_{is\infty}(\gamma, 0) = 1$ for $i=c, e, a$ is completely independent of γ for all models. The functions $f_{od}(\gamma, 0)$ and $f_{is\epsilon}(\gamma, 0)$ for $\epsilon=0$ and 1 are

compared in Fig. 3, where they are plotted as functions of $1/\gamma$ for clarity. Clearly, for $\epsilon \geq 1$, $f_{is\epsilon}(\gamma, 0)$ is nearly independent of γ , which also implies $J_{c, is\epsilon}^J(\gamma, \phi_0)$ is nearly independent of ϕ_0 for $\epsilon \geq 1$.

For the $d_{x^2-y^2}$ -wave OP's, $J_{c, id\epsilon}^J(\gamma, \phi_0)/J_{c, s}^J = f_{id\epsilon}(\gamma, \phi_0)$ at T_c . Again, $f_{id\epsilon}(\gamma, \pm\pi/2 - \phi_0) = f_{id\epsilon}(\gamma, \phi_0)$. The γ and ϕ_0 dependencies of the $f_{id\epsilon}(\gamma, \phi_0)$ are shown in Figs. 3, 5, and 6. For the anomalous- $d_{x^2-y^2}$ -wave case with the four rotationally invariant tunneling models, $f_{ad\epsilon}(\gamma, \phi_0) = [(2\epsilon + 1)^2 f_2(\gamma) \cos(2\phi_0) + f_6(\gamma) \cos(6\phi_0)]/[8(1 + |\epsilon|^2)]$. For the Lorentzian model, $f_{ad\epsilon}(\gamma, \phi_0) = [(A + C) \cos(2\phi_0) + (B + C) \cos(6\phi_0)]/[8(1 + |\epsilon|^2)]$, where $A = (2\epsilon + 1)^2 [f_{2,0}^L(\gamma) + f_{0,1}^L(\gamma)]$, $B = 4[f_{6,0}^L(\gamma) + f_{0,3}^L(\gamma)]$, and $C = 2(\epsilon + 1)[f_{2,2}^L(\gamma) + f_{4,1}^L(\gamma)]$. Hence, for all five models, $f_{ad\epsilon}(\gamma, \phi_0)$ clearly vanishes at $\phi_0 = \pi/4$ for all ϵ, γ values. In the coherent limit for all four rotationally invariant tunneling models, this approaches $[(2\epsilon + 1)^2 \cos(2\phi_0) + \cos(6\phi_0)]/[8(1 + |\epsilon|^2)]$. For the Lorentzian model, the coefficients are slightly different, as found from Eq. (B19) in Appendix B. As $\gamma \rightarrow 0$, $f_{ad\epsilon}(0, \phi_0) \rightarrow 0$. The exponential model gives the slowest approach to zero, for both the $\cos(2\phi_0)$ and $\cos(6\phi_0)$ terms, of all five models.

For the $i = c, e$ $d_{x^2-y^2}$ -wave OP models as $\epsilon \rightarrow 0$ for all four rotationally invariant tunneling models in the coherent limit, $f_{ed0}(\infty, \phi_0) = [\frac{3}{2} |\sin(4\phi_0)| + (\pi - 4|\phi_0|) \cos(4\phi_0)]/(4\pi)$ and $f_{cd0}(\infty, \phi_0) = [|\sin(4\phi_0)| + (\pi - 4|\phi_0|) \cos(4\phi_0)]/(8\pi)$. Although these functions both vanish at $\pi/4$, they are not equivalent, as $f_{ed0}(\infty, 0) = \frac{3}{8}$, but $f_{cd0}(\infty, 0) = \frac{1}{8}$, as seen in Fig. 5. This difference at $\phi_0 = 0$ arises from the anisotropy of the $\tilde{\psi}_{is0}(\phi_{\mathbf{k}})$ relative to that of $\tilde{\psi}_{od}(\phi_{\mathbf{k}})$ present in the $\tilde{\psi}_{id0}(\phi_{\mathbf{k}})$. In Fig. 6, we show the ϕ_0 dependence of the rotationally invariant coherent limit $f_{id0}(\infty, \phi_0)$, along with the $|\cos(2\phi_0)|$ behavior obtained for the $d_{x^2-y^2}$ -wave OP. We also show the results for the coherent limit in the Lorentzian model, which are indicated by the open diamonds. We note that for the $d_{x^2-y^2}$ -wave OP, the Lorentzian tunneling results for $J_{c, od}^J(\phi_0)/J_{c, od}^J(0)$ are indistinguishable from those of the rotationally invariant models. This is somewhat remarkable, as the magnitudes of $J_{c, od}^J(0)$ are not identical. For the compressed- and extended- $d_{x^2-y^2}$ -wave OP's, however, the identical ϕ_0 dependence of $J_{c, id\epsilon}^J$ obtained with the Lorentzian model is somewhat different from that obtained from the rotationally invariant tunneling models. As $\gamma \rightarrow 0$, both of the $f_{id\epsilon}(0, \phi_0) \rightarrow 0$. Again, the exponential model has the slowest decay to zero. Regardless of ϵ, γ , $f_{id\epsilon}(\gamma, \pi/4) = 0$.

In the coherent limit, except for the Lorentzian model, $f_{as\epsilon}(\infty, 0) \rightarrow (\epsilon^2 + 1/2)/(1 + |\epsilon|^2)$ and for $i = c, e$, $f_{is\epsilon}(\infty, 0) \rightarrow [(1/2 + \epsilon^2)/(1 + \epsilon^2)]$ for arbitrary ϵ . These results interpolate smoothly and monotonically between 1/2 and 1 as $\epsilon \rightarrow 0$ and as $\epsilon \rightarrow \infty$, respectively. For other values of ϕ_0 and γ , we resort to numerical evaluations. For the Lorentzian model in the coherent limit, the coefficients $f_{n,m}^L(\gamma \rightarrow \infty)$ are given in Appendix B. Numerically, we find $f_{es0}(\infty, 0) \rightarrow 0.530$, $f_{cs0}(\infty, 0) \rightarrow 0.465$, but at $\phi_0 = \pi/4$, $f_{cs0}(\infty, \pi/4) = f_{es0}(\infty, \pi/4) = 0.3175$. For the $d_{x^2-y^2}$ -wave functions, $f_{ed0}(\infty, 0) \rightarrow 0.406$, $f_{cd0}(\infty, 0) \rightarrow 0.121$, but they both satisfy $f_{id0}(\infty, \pi/4) = 0$, as required by the theorem.

It is a curious feature of the Lorentzian model that the coherent limits obtained for the d -wave and extended- s -wave models are not precisely the same as those obtained by letting $f^J(\phi_{\mathbf{k}}, \phi_{\mathbf{k}'}) \propto \delta(\phi_{\mathbf{k}} - \phi_{\mathbf{k}'})$. This detail is not present in the tight-binding Lorentzian model, Eq. (37). In that case, the Lorentzian model is an effective smearing of the two-dimensional δ function, $\delta^{(2)}(\mathbf{k} - \mathbf{k}')$, which provides two relations between the four momentum variables. For circular Fermi-surface-restricted pairings, there are only two variables $\phi_{\mathbf{k}}$ and $\phi_{\mathbf{k}'}$, which again must satisfy two relations present in the Lorentzian model, especially in the coherent limit. Hence, this overrestriction leads to a spurious slight excess in the coherent critical current.

For all γ values and for any type of time-reversal-invariant tunneling, an ordinary- $d_{x^2-y^2}$ -wave OP proportional to $\cos(2\phi_{\mathbf{k}})$ satisfies $J_{c, od}^J(\phi_0) \propto |\cos(2\phi_0)|$, which vanishes at $\phi_0 = 45^\circ$, as shown in Fig. 6. Other $d_{x^2-y^2}$ -wave forms, while containing contributions to $J_{c, id\epsilon}^J$ of the form $\cos[(4n+2)\phi_0]$, closely approximate the simple form $|\cos(2\phi_0)|$, and always vanish at $\phi_0 = 45^\circ$. On the other hand, $J_{c, is\epsilon}(\gamma, \phi_0)$ for a general- s -wave superconductor is very unlikely to vanish at $\phi_0 = \pi/4$, and in the incoherent limit, $f_{is\epsilon}(\gamma, \phi_0) \rightarrow d_{is0}^2(\epsilon)$, a constant. This constant is nonvanishing except for the fully anomalous OP, $\Delta_{as0}(\phi_{\mathbf{k}}) = \Delta_0 \cos(4\phi_{\mathbf{k}})$, but in that particular case $J_{c, as0}^J(\gamma, \phi_0) \propto |\cos(4\phi_0)|$, and in the incoherent limit, $f_{as0}(0, \phi_0) = 0$, just as all of the $f_{id\epsilon}(0, \phi_0) = 0$. But, $f_{as0}(\gamma, \phi_0)$ vanishes at $\phi_0 = \pi/8$, and not at $\pi/4$, as seen in Fig. 6. Thus, even an s -wave OP which averages to 0 over the Fermi surface can be distinguished from a general- $d_{x^2-y^2}$ -wave OP in the c -axis twist experiment.

B. Tight-binding Fermi-surface models

We calculated $J_{c, i\zeta\epsilon}^J(\sigma, \phi_0)$ in the standard BCS model of superconductivity, assuming a phenomenological pairing interaction which gives an OP of one of the forms, Eqs. (8)–(15), for each of the five tunneling models presented in Eqs. (34)–(39). For simplicity, we limit our presentation to the case $T \rightarrow T_c$, since results for the Monthoux-Pines-like pairing models with the Gaussian tunneling model at $T = 0.5T_c$ and $0.9T_c$ were shown elsewhere.⁵⁷ In Figs. 7–13, we presented our results for the ordinary-, extended-, compressed-, and anomalous- s - and $d_{x^2-y^2}$ -wave OP's with $\epsilon = 0$. Results for intermediate values of ϵ , such as $\epsilon = 1$, are intermediate between the $\epsilon = 0$ and $\epsilon \rightarrow \infty$ cases presented, and are omitted for brevity of presentation.

We calculated $J_{c, i\zeta\epsilon}^J(\sigma, \phi_0)$ from Eq. (1), where just below T_c , we set $F_\omega(\mathbf{k}) = \Delta(\mathbf{k}, T)/[\omega^2 + \xi^2(\mathbf{k})]$ and $F_\omega^\dagger(\tilde{\mathbf{k}}') = F_\omega(\tilde{\mathbf{k}}')$ inside the argument of the absolute value sign. In each figure, the curves representing the results for the Gaussian, exponential, rotationally invariant Lorentzian, stretched Lorentzian, and Lorentzian models are tagged with solid circles, open circles, open triangles, inverted solid triangles, and open diamonds, respectively. In addition, results for the σ^2 values 0.0005, 0.005, 0.05, and 0.20 are shown with solid, dotted, dashed, and dot-dashed curves, respectively, except that for the anomalous OP's, the solid curves repre-

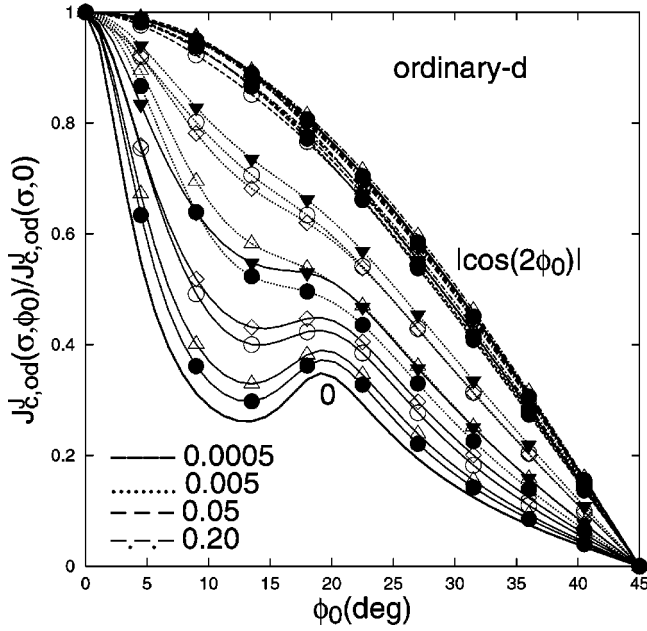


FIG. 7. Plots of $J_c^I(\phi_0)/J_c^I(0)$ just below T_c for twist junctions with the Fermi surface shown in Fig. 1, and an ordinary- $d_{x^2-y^2}$ -wave OP, $\Delta_0(T)\psi_{od}(\mathbf{k})$, Eq. (12). The dimensionless parameter σ^2 values 0.0005, 0.005, 0.05, and 0.20 are indicated by the thin solid, dotted, dashed, and dot-dashed curves, respectively. The thick curves correspond to the coherent ($\sigma^2=0$) limit and the function $|\cos(2\phi_0)|$, as indicated. Results for the Gaussian (solid circles), exponential (open circles), rotationally invariant Lorentzian (open triangles), stretched Lorentzian (solid inverted triangles), and Lorentzian (open diamonds) tunneling models are shown.

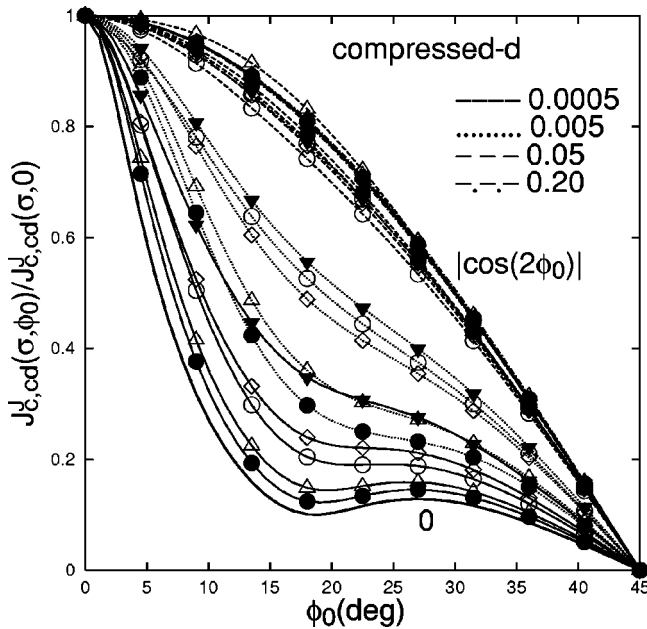


FIG. 8. Plots of $J_c^I(\phi_0)/J_c^I(0)$ just below T_c for twist junctions with the Fermi surface shown in Fig. 1 and a compressed- $d_{x^2-y^2}$ -wave OP, $\Delta_0(T)\psi_{cd}(\mathbf{k})$, Eq. (14), with $\epsilon=0$. The curve types and symbols are the same as in Fig. 7.

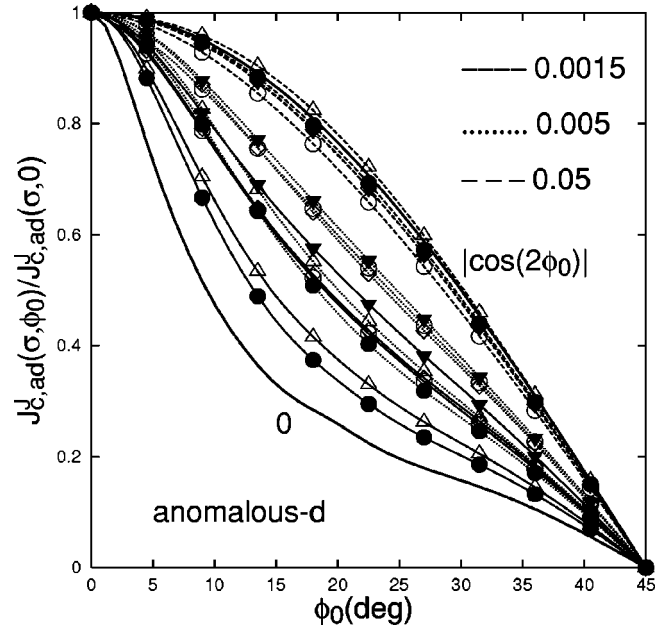


FIG. 9. Plots of $J_c^I(\phi_0)/J_c^I(0)$ just below T_c for twist junctions with the Fermi surface shown in Fig. 1 and an anomalous- $d_{x^2-y^2}$ -wave OP, $\Delta_0(T)\psi_{ad}(\mathbf{k})$, Eq. (15). The curve types and symbols are the same as in Fig. 7, except that curves for $\sigma^2=0.20$ are not shown.

sent $\sigma^2=0.0015$. We also present the results for the coherent limit $\sigma^2=0$ as the thick solid curves labeled 0. For the $d_{x^2-y^2}$ -wave OP's, the function $|\cos(2\phi_0)|$ is shown in Figs. 7–9 as a thick solid curve for comparison. For the extended-

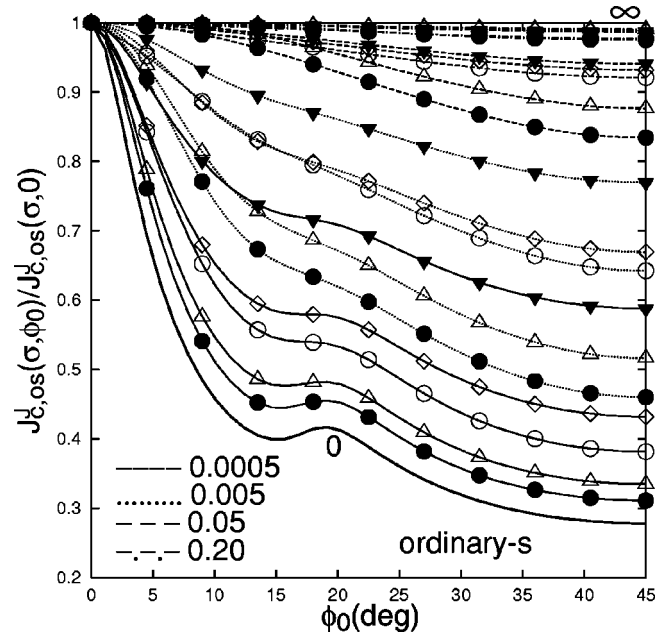


FIG. 10. Plots of $J_c^I(\phi_0)/J_c^I(0)$ just below T_c for twist junctions with the Fermi surface shown in Fig. 1 and an ordinary- s -wave OP, $\Delta_0(T)\psi_{os}(\mathbf{k})$, a constant. The thick curves correspond to the coherent ($\sigma^2=0$) and incoherent ($\sigma^2=\infty$, unity) limits. The thin-curve types and symbols are the same as in Fig. 7. For clarity, the vertical axis begins at 0.2.

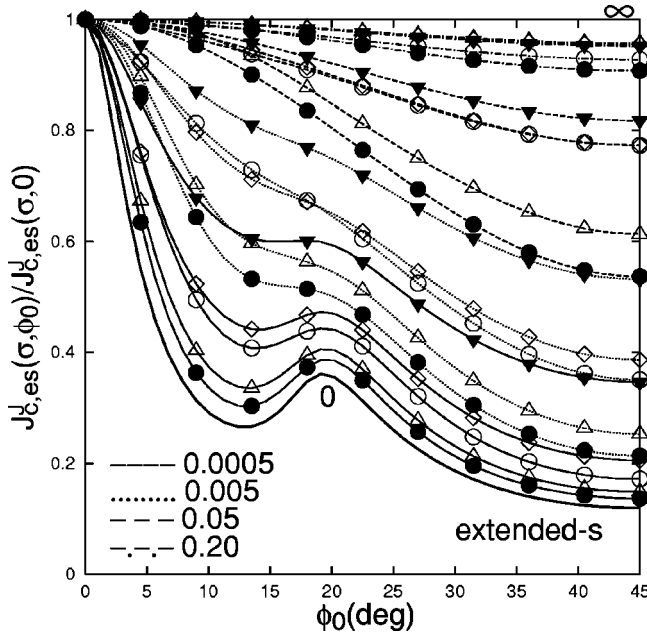


FIG. 11. Plots of $J_c^J(\phi_0)/J_c^J(0)$ just below T_c for twist junctions with the Fermi surface shown in Fig. 1 and an extended- s -wave OP, $\Delta_0(T)\psi_{es0}(\mathbf{k})$, Eq. (9) with $\epsilon=0$. The curve types and symbols are the same as in Fig. 10.

d -wave OP, the peak for coherent tunneling at $\phi_0 \approx 20^\circ$ is somewhat stronger than that pictured in Fig. 7. Otherwise, curves for the extended- d -wave OP are nearly indistinguishable from those of the ordinary- d -wave OP, Fig. 7, and are omitted for brevity. Results for the general- s -wave OP's are

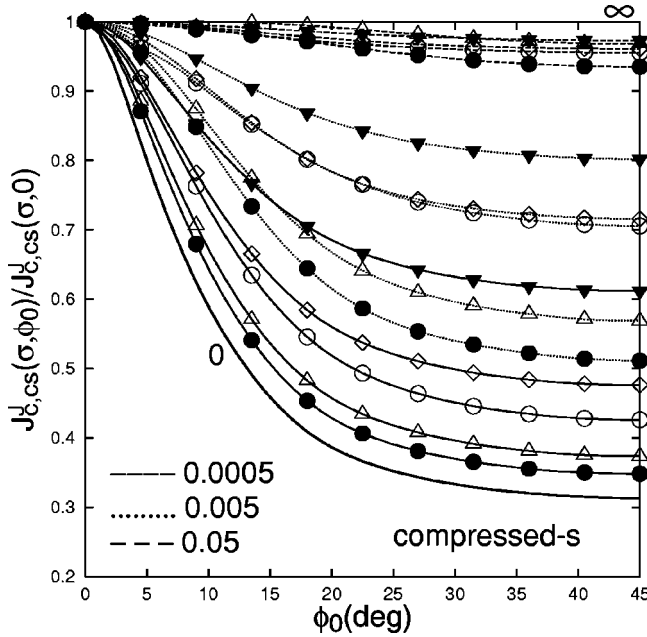


FIG. 12. Plots of $J_c^J(\phi_0)/J_c^J(0)$ just below T_c for twist junctions with the Fermi surface shown in Fig. 1 and a compressed- s -wave OP, $\Delta_0(T)\psi_{cs0}(\mathbf{k})$, Eq. (10), with $\epsilon=0$. The curve types and symbols are the same as in Fig. 10, except that curves for $\sigma^2=0.20$ are not shown.

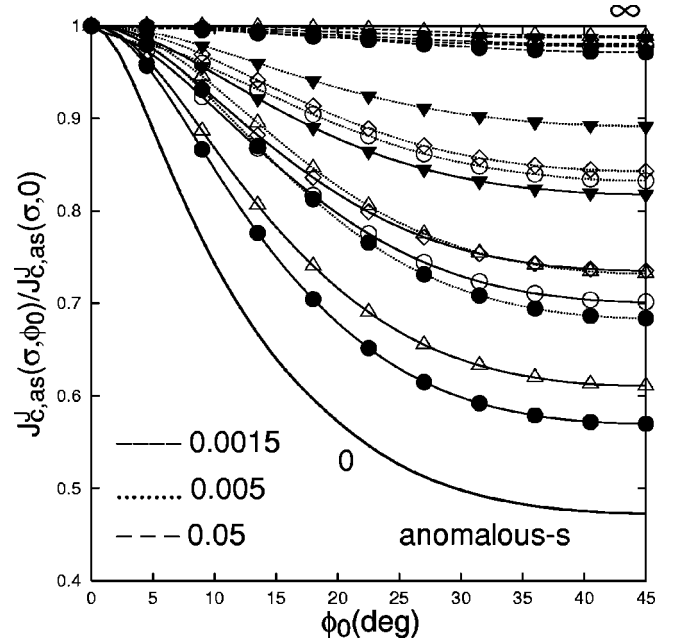


FIG. 13. Plots of $J_c^J(\phi_0)/J_c^J(0)$ just below T_c for twist junctions with the Fermi surface shown in Fig. 1 and an anomalous- s -wave OP, $\Delta_0(T)\psi_{as}(\mathbf{k})$, Eq. (11). The curve types and symbols are the same as in Fig. 10, except that curves for $\sigma^2=0.20$ are not shown.

pictured in Figs. 10–13. In these figures, we label the incoherent limit $J_{c,ise}^J(\infty, \phi_0)/J_{c,ise}^J(\infty, 0) = 1$ at the figure boundary by the symbol ∞ .

For each OP, coherent tunneling causes $J_c^J(\sigma, \phi_0)/J_c^J(\sigma, 0)$ to decrease sharply as ϕ_0 increases from 0° .⁴¹ This occurs because the overlap of the tight-binding Fermi surfaces changes dramatically from a continuous curve for $\phi_0=0$ to a set of four points for $\phi_0>0^\circ$.

In comparing Figs. 7–9 for OP's with general- d -wave symmetry, we first see that they all obey the theorem requiring $J_{c,ide}^J(\sigma, \pi/4) = 0$. This is contrasted sharply with the behavior of the general- s -wave OP's, shown in Figs. 10–13. In those figures, $J_{c,s}^J(\sigma, \pi/4)$, while often smaller than $J_{c,s}^J(\sigma, 0)$, is always finite. In addition, we see that for Figs. 7, 8, 10, and 11, and also for the unpictured results for the extended- d -wave OP, the precise details of the Fermi surface give rise to a prominent peak in $J_{c,i\zeta\epsilon}^J(\sigma, \phi_0)$ at $\phi_0 = \phi_0^* \approx 20^\circ$ in the coherent limit. In these figures, this peak arises when the rotated Fermi surfaces intersect at eight points, instead of just four for $\phi_0 < \phi_0^*$. However, in Figs. 9, 12, and 13, the anomalous- $d_{x^2-y^2}$ -wave and compressed- and anomalous- s -wave OP's yield somewhat different results. In these cases, the parts of the Fermi surface that play the dominant role in this peak effect are those nearest to the edge of the Brillouin zone, where these OP's vanish. Thus, we obtain instead a smooth curve, which flattens for large twist angles. This arises from a complicated mix of the Fermi surface and OP anisotropy.

For tunneling that is nearly coherent, $\sigma^2 < 0.005$, we see in each of these seven figures that the coherent limit results for $J_{c,i\zeta\epsilon}^J(\sigma, \phi_0)/J_{c,i\zeta\epsilon}^J(\sigma, 0)$ are most closely approximated by the Gaussian tunneling model, followed by the rotation-

ally invariant Lorentzian, the exponential, the Lorentzian, and the stretched Lorentzian models. This order is nearly maintained for $\sigma^2=0.005$, although in Fig. 7, there is a slight change in the order of the results from the Lorentzian and exponential tunneling models for $\phi_0 < \phi_0^*$. For $\sigma^2=0.0005$, the peak in $J_{c,i\xi\epsilon}^J(\phi_0)$ at ϕ_0^* is still evident in Figs. 7, 8, 10, and 11, although in the stretched Lorentzian model, it has been smeared out the most, having been reduced to a shoulder in some of the figures. For $\sigma^2=0.005$, the peak at ϕ_0^* has been reduced to a shoulder at best in Figs. 7, 8, 10, and 11.

As for Fig. 6, we see that in Figs. 7–9 for the various general- $d_{x^2-y^2}$ -wave models, the $\sigma^2=0.05$ curves differ from $|\cos(2\phi_0)|$ by less than 10%, and the $\sigma^2=0.2$ results are almost indistinguishable from it. In Fig. 7, the differences are barely perceptible. But, in Fig. 8, the compressed- $d_{x^2-y^2}$ -wave OP results for $\sigma^2=0.2$ fall within the width of the thick solid line representing $|\cos(2\phi_0)|$. Although not pictured, this is also true for the anomalous- $d_{x^2-y^2}$ -wave OP results. The approach to the incoherent limit for the $d_{x^2-y^2}$ -wave OP's depends somewhat upon the particular tunneling model. For $\sigma^2=0.05$ and 0.2, the order of the results obtained with the various tunneling models has been altered from that near the coherent limit, but differently in each figure. Most prominent is the curve for $\sigma^2=0.2$ obtained with the rotationally invariant Lorentzian model and the compressed- $d_{x^2-y^2}$ -wave OP, which actually lies above the $|\cos(2\phi_0)|$ curve. Likewise, for the general- s -wave models, Figs. 10 – 13 show that for $\sigma^2=0.05$ and 0.2, the order of the results obtained with the different models has been altered somewhat from that near the coherent limit. Although the Gaussian results still lie below the others, the order of increasing $J_{c,i\xi\epsilon}^J(\sigma, \phi_0)/J_{c,i\xi\epsilon}^J(\sigma, 0)$ is now Gaussian, exponential, Lorentzian, stretched Lorentzian, and finally rotationally invariant Lorentzian.

We remark that for the ordinary- s -wave OP, Fig. 10 shows that all of the $\sigma^2=0.2$ curves are consistent with the data of Li *et al.*, and the curves for $\sigma^2=0.05$ are generally inconsistent with the data, although the exponential, Lorentzian, and stretched Lorentzian models give results that differ from the data by only one standard deviation.⁸ For the extended- s -wave OP, however, Fig. 11 shows that all of the $\sigma^2=0.05$ curves are inconsistent with the data, but the $\sigma^2=0.2$ curves for the rotationally invariant Lorentzian and stretched Lorentzian models are consistent with the data of Li *et al.*, with the other tunneling models giving results that are only marginally consistent with the data for $\sigma^2=0.2$. However, Figs. 12 and 13 show that the compressed- and anomalous- s -wave OP's are less sensitive to the amount of tunneling incoherence than are the other general- s -wave OP's. In this case, all of the curves for $\sigma^2=0.2$ are rather indistinguishable from unity, and thus cannot be excluded. Furthermore, the curves for $\sigma^2=0.05$ are at least marginally consistent with the data, and for the stretched and rotationally invariant Lorentzian tunneling models are within one standard deviation of the data. In any event, one must have a general- s -wave OP symmetry to fit the data, and the tunneling must be very nearly incoherent, with $\sigma^2 \geq 0.05$. As seen from Fig. 1, this implies that the change in parallel wave

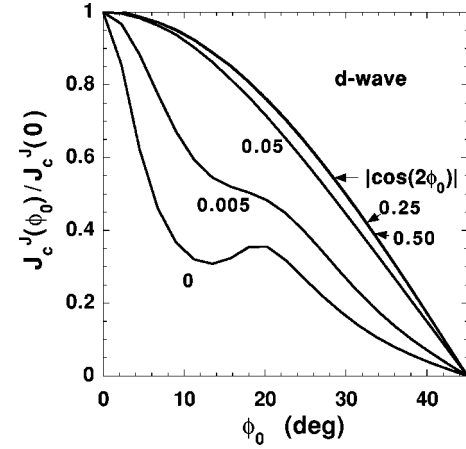


FIG. 14. Plots of $J_c^J(\phi_0)/J_c^J(0)$ at $T/T_c=0.5$ for Gaussian twist junctions with the Fermi surface shown in Fig. 1, and a $d_{x^2-y^2}$ -wave OP obtained from the Monthoux-Pines pairing model. The Gaussian dimensionless parameters σ^2 values are indicated. Curves for $\sigma^2=0.25$ and 0.50 are nearly indistinguishable from the incoherent limit function $|\cos(2\phi_0)|$.

vector of the quasiparticles involved in the tunneling must cover a substantial fraction (7%) of the first BZ.

For the Monthoux-Pines-like pairing models leading to the ordinary- d -wave, extended- s -wave and ordinary- s -wave OP's, we previously performed explicit calculations of $J_c^J(\phi_0)$ at $T/T_c=0.5, 0.9$, with the Gaussian tunneling model, Eq. (34).⁵⁷ In Fig. 14, we normalized those results for the $d_{x^2-y^2}$ -wave OP at $T=0.5T_c$ relative to its value at $\phi_0=0$, for comparison with the results shown in Figs. 7–13. It is easily seen that the curves in Fig. 14 are nearly indistinguishable from the respective Gaussian tunneling curves for the ordinary- d -wave OP just below T_c , pictured in Fig. 7. Similarly, the analogous curves for the Monthoux-Pines-like extended- s OP at $0.5T_c$ are nearly indistinguishable from the respective Gaussian curves just below $T=T_c$, pictured in Fig. 11. Results for the ordinary- s -wave OP are slightly different from the Gaussian curves pictured in Fig. 10, with the largest difference being in the coherent limit at $\phi_0=45^\circ$, where the unpictured result has the value 0.35. The general shapes of the curves are otherwise nearly indistinguishable from those pictured in Fig. 10, and hence for brevity these extended- and ordinary- s -wave results are not pictured. We remark that going to lower- T values does not change anything qualitatively. The criteria for the twist theorem to hold do not involve the temperature, as long as it is below T_c , so that the critical current for a superconductor with general- d -wave symmetry must vanish at $\phi_0=0$. The only changes that we expect are thus small ones for the general- s -wave OP forms.

The fact that our results for OP forms with somewhat different wave-vector dependencies are so similar is important. This demonstrates that the dominant contributions to the c -axis tunneling arise from pairing in the regions in the first BZ nearest to the Fermi surface. Thus, we expect that any models which also involve pairing away from the Fermi surface should not differ substantially from those presented

here, as long as their projections onto the Fermi surface are similar to those of the OP forms studied here.

IV. THE INCOHERENT LIMIT

We now discuss in detail the approach to the incoherent limit for c -axis twist junctions involving a $d_{x^2-y^2}$ -wave superconductor. For each of the five models we have considered, we have characterized the crossover from the coherent to the incoherent limits with a single parameter $\tilde{\sigma}$. As $\tilde{\sigma} \rightarrow \infty$, $f^J(\mathbf{k}-\mathbf{k}') \rightarrow 1/\tau_\perp$, a constant. Thus, for there to be any coupling between two $d_{x^2-y^2}$ -wave superconductors, $f^J(\mathbf{k}-\mathbf{k}')$ must depend upon $\mathbf{k}-\mathbf{k}'$. In the circular Fermi-surface model, this can be incorporated by letting $f^J(\phi_{\mathbf{k}}-\phi_{\mathbf{k}'}) = 1/\tau_{\perp s} + 1/\tau_{\perp d} \cos[2(\phi_{\mathbf{k}}-\phi_{\mathbf{k}'})]$.^{25,53-56} However, it is elementary to show that this model leads to $J_{c, is\epsilon}^J(\phi_0) \propto 1/\tau_{\perp s}$ and $J_{c, id\epsilon}^J(\phi_0) \propto |\cos(2\phi_0)|/\tau_{\perp d}$, even for the most general- s - and $d_{x^2-y^2}$ -wave OP forms given by Eqs. (30) and (31), respectively. For more general forms of $f^J(\phi_{\mathbf{k}}-\phi_{\mathbf{k}'})$, the critical current just below T_c is given by Eqs. (54)–(58) for arbitrary γ , including the incoherent limit $\gamma \rightarrow 0$.

A similar statement can be made for the tight-binding band, as well. We assume that $f^J(\mathbf{k}-\mathbf{k}')$ is rotationally invariant. As the incoherent limit is approached, we then assume

$$f^J(\mathbf{k}-\mathbf{k}') \rightarrow [1 - c_\mu |(\mathbf{k}-\mathbf{k}')/\tilde{\sigma}|^\mu]/\tau_\perp, \quad (59)$$

where c_μ is a dimensionless constant of order unity. In the models discussed here, $\mu = 1, 2, 4$, but we can generally allow μ to be any positive real number. We then write $\tau_\perp f^J(\mathbf{k}-\mathbf{k}') - 1$ in terms of a Taylor series in $\mathbf{k} \cdot \mathbf{k}'$, which does not terminate unless μ is an even integer,

$$\tau_\perp f^J(\mathbf{k}-\mathbf{k}') - 1 \rightarrow -c_\mu \left[\frac{(k^2 + k'^2)}{\tilde{\sigma}^2} \right]^{\mu/2} \sum_{l=0}^{\infty} \left(\frac{2\mathbf{k} \cdot \mathbf{k}'}{k^2 + k'^2} \right)^{2l} A_{l\mu}, \quad (60)$$

where

$$A_{l\mu} = \frac{\Gamma(\mu/2 + 1)}{\Gamma(\mu/2 - 2l + 1)(2l)!} \quad (61)$$

and $\Gamma(x)$ is the gamma function. Some features of the $A_{l\mu}$ are discussed in Appendix C. We have kept only terms with even powers of $\mathbf{k} \cdot \mathbf{k}'$, as the terms with odd powers are only appropriate for triplet superconductors. Since our numerical calculations have shown that it makes essentially no difference if one includes umklapp processes or not, we are free to include the wave vectors that appear in only one of the first BZ's on an equal basis with those that appear in both first BZ's. Now, it is simplest to do the integral in Eq. (1) in the following way. We let the integration variables be \mathbf{k} and $\tilde{\mathbf{k}}'$. Then, we rotate the variables $\tilde{\mathbf{k}}'$ and \mathbf{k}' in $f^J(\mathbf{k}-\mathbf{k}')$ by $-\phi_0$ about the c axis, relative to the $\tilde{\mathbf{k}}'$. Now, the integration variables are just \mathbf{k} and \mathbf{k}' instead of rotated ones. We then *redefine* \mathbf{k} and \mathbf{k}' to be the wave vectors in the F functions in Eq. (1), and let $\tilde{\mathbf{k}} = \mathbf{k}$ and $\tilde{\mathbf{k}}'$ be these rotated wave vectors in

f^J . Since $\tilde{k}^2 + \tilde{k}'^2 = k^2 + k'^2$ is invariant under such rotations, the only quantity in Eq. (60) which is altered by the rotation is $\mathbf{k} \cdot \mathbf{k}'$, which becomes

$$\tilde{\mathbf{k}} \cdot \tilde{\mathbf{k}}' = kk' \cos(\phi_{\mathbf{k}} - \phi_{\mathbf{k}'} - \phi_0), \quad (62)$$

where we used polar coordinates, $\mathbf{k} = k(\cos \phi_{\mathbf{k}}, \sin \phi_{\mathbf{k}})$, etc. It is then straightforward to show that the general- s - and $d_{x^2-y^2}$ -wave critical current densities, for arbitrary $T \leq T_c$, and an arbitrary tetragonal Fermi surface, near the incoherent limit of an arbitrary tunneling matrix element squared, reduce to

$$J_{c, s}^J(\sigma, \phi_0, T) \xrightarrow{\sigma \gg 1} \left[\frac{4eT}{\tau_\perp} \sum_{\omega} \left[\Pi_{s0}^{00}(\omega) - \frac{c_\mu}{\tilde{\sigma}^\mu} \sum_{l=0}^{\infty} A_{l\mu} \right. \right. \\ \left. \left. \times \sum_{m=0}^{E(l/2)} C_{slm} \Pi_{s\mu}^{lm}(\omega) \cos(4m\phi_0) \right] \right] \quad (63)$$

and

$$J_{c, d}^J(\sigma, \phi_0, T) \xrightarrow{\sigma \gg 1} \left[\frac{4eT}{\tau_\perp} \sum_{\omega} \frac{(-c_\mu)}{\tilde{\sigma}^\mu} \sum_{l=1}^{\infty} A_{l\mu} \right. \\ \left. \times \sum_{m=0}^{E[(l-1)/2]} C_{dlm} \Pi_{d\mu}^{lm}(\omega) \cos[(4m+2)\phi_0] \right], \quad (64)$$

where

$$\Pi_{s\mu}^{lm}(\omega) = \langle F_\omega(\mathbf{k}) F_\omega(\mathbf{k}') S^{lm}(\mathbf{k}) S^{lm}(\mathbf{k}') (k^2 + k'^2)^{\mu/2 - 2l} \rangle, \quad (65)$$

$$\Pi_{d\mu}^{lm}(\omega) = \langle F_\omega(\mathbf{k}) F_\omega(\mathbf{k}') D_{x^2-y^2}^{lm}(\mathbf{k}) D_{x^2-y^2}^{lm}(\mathbf{k}') \\ \times (k^2 + k'^2)^{\mu/2 - 2l} \rangle, \quad (66)$$

$E(x)$ is the integer function, and the constants C_{slm} and C_{dlm} and the ‘‘tunnel functions’’ $S^{lm}(\mathbf{k})$ and $D_{x^2-y^2}^{lm}(\mathbf{k})$ of s - and $d_{x^2-y^2}$ -wave symmetry, respectively, are given in Appendix C. There we list the tunnel functions for all (l, m) in polar coordinates and for $l \leq 4$ in rectangular coordinates, and also present some details of the calculation. Equations (65) and (66) are evaluated in rectangular coordinates over the first BZ, using the tight-binding quasiparticle dispersion, Eq. (2), and the appropriate particular choice of the OP's in Eqs. (8)–(15) under study.

We rewrite Eqs. (63) and (64) as

$$J_{c, is\epsilon}^J(\sigma, \phi_0, T) \xrightarrow{\sigma \gg 1} \left| \sum_{n=0}^{\infty} b_{isn}(\epsilon, \sigma, T) \cos(4n\phi_0) \right| \quad (67)$$

and

$$J_{c, id\epsilon}^J(\sigma, \phi_0, T) \xrightarrow{\sigma \gg 1} \left| \sum_{n=0}^{\infty} b_{idn}(\epsilon, \sigma, T) \cos[(4n+2)\phi_0] \right|, \quad (68)$$

which defines the coefficients b_{isn} and b_{idn} . The $n=0$ term $b_{is0}(\epsilon, \sigma, T)$ is the only nonvanishing coefficient in the incoherent limit. Although all of the $b_{idn}(\epsilon, \sigma, T)$ vanish as $\sigma \rightarrow \infty$, the dominant one for $\sigma \gg 1$ is the $n=0$ term, $b_{id0}(\epsilon, \sigma, T)$. For most tunneling models, $b_{isn}(\epsilon, \sigma, T)$ and $b_{idn}(\epsilon, \sigma, T)$ can be shown to be of increasing order in σ^{-2} as n increases.

For the Gaussian and the stretched Lorentzian tunneling models, the leading correction to a constant f^J has $\mu=2$ in Eq. (59) near the incoherent limit. For a $d_{x^2-y^2}$ -wave superconductor, the $\mu=2$ term leads to a vanishing $J_{c,ide}^J(\sigma, \phi_0, T)$ for all ϕ_0 , so one needs to go to the next order, $\mu=4$. The resulting leading term is proportional to $|\cos(2\phi_0)|$. In these cases, $c_4 < 0$, as in a $d_{x^2-y^2}$ -wave scattering model.⁵⁴ For the rotationally invariant Lorentzian tunneling model, the leading correction has $\mu=4$. For a $d_{x^2-y^2}$ -wave superconductor, the leading contribution to $J_{c,ide}^J$ is again proportional to $|\cos(2\phi_0)|$. However, $c_4 > 0$, so that the model simulates a π junction between $d_{x^2-y^2}$ -wave superconductors for $\phi_0=0$, as one approaches the incoherent limit.

The more complicated cases are the models in which Eq. (60) applies with $0 < \mu < 2$, such as $\mu=1$ for the exponential model. In such cases, all terms in the expansion contribute to the leading correction to f^J . For $0 < \mu < 2$, $c_\mu > 0$, and $A_{0\mu} = 1$, but the remaining $A_{l\mu} < 0$, leading to results consistent with the s - and $d_{x^2-y^2}$ -wave scattering model.⁵⁴ In the exponential model, the leading contributions to the $b_{isn}(\epsilon, \sigma, T)$ for $n \geq 1$ (subsequent to the constant $n=0$ term) and to all of the $b_{idn}(\epsilon, \sigma, T)$ for $n \geq 0$ are all of the same order in σ^{-2} . Numerically, the exponential model doesn't appear to be much different than the other models for the rather large σ^2 value of 0.05. The differences in $J_{c,ide}^J(\sigma, \phi_0, T)$ between the four rotationally invariant tunneling models for the various $d_{x^2-y^2}$ -wave OP models we considered are only a few percent for $\sigma^2=0.5$, and all are very close to $|\cos(2\phi_0)|$. Although this is not obvious for the exponential model, at least in the circular Fermi-surface model, the contributions of order $\cos[(4n+2)\phi_0]$ fall off rapidly with increasing n , as seen from Eq. (56) and Eq. (B10) of Appendix B.

We now consider the Lorentzian model, which is not rotationally invariant. Expanding $f_L^J(\tilde{\mathbf{k}} - \tilde{\mathbf{k}}')$ near the incoherent limit, we have

$$f_L^J(\tilde{\mathbf{k}} - \tilde{\mathbf{k}}') = f_{0L}^J \{ 1 - (\tilde{\mathbf{k}} - \tilde{\mathbf{k}}')^2 / \tilde{\sigma}^2 + [(\tilde{\mathbf{k}} - \tilde{\mathbf{k}}')^4 - (\tilde{k}_x - \tilde{k}_x')^2 (\tilde{k}_y - \tilde{k}_y')^2] / \tilde{\sigma}^4 + \dots \}. \quad (69)$$

Clearly, the leading terms for a $d_{x^2-y^2}$ -wave superconductor are proportional to $4(\tilde{\mathbf{k}} \cdot \tilde{\mathbf{k}}')^2 - (\tilde{k}_x - \tilde{k}_x')^2 (\tilde{k}_y - \tilde{k}_y')^2$. The $(\tilde{\mathbf{k}} \cdot \tilde{\mathbf{k}}')^2$ term is given in Appendix C. The remaining part diagonal in the $d_{x^2-y^2}$ -wave tunnel functions is $\frac{1}{2} \cos(2\phi_0) D_{x^2-y^2}^{10}(\mathbf{k}) D_{x^2-y^2}^{10}(\mathbf{k}')$. Taken together, the dominant part of $f_L^J(\tilde{\mathbf{k}} - \tilde{\mathbf{k}}')$ which contributes to $J_{c,ide}^J(\sigma, \phi_0, T)$ is $f_{0L}^J \frac{5}{2} \cos(2\phi_0) D_{x^2-y^2}^{10}(\mathbf{k}) D_{x^2-y^2}^{10}(\mathbf{k}') / \tilde{\sigma}^4$, implying $c_4 < 0$. Hence, $J_{c,ide}^J(\sigma, \phi_0, T) \propto |\cos(2\phi_0)|$ as the incoherent limit is approached.

Thus, the extreme incoherent limit gives the most profound difference between a general- s -wave superconductor and a general- $d_{x^2-y^2}$ -wave superconductor. Independent of the details of the tunneling, the shape of the Fermi surface, and the precise form of the OP's,

$$\lim_{\sigma \rightarrow \infty} [J_{c,ise}^J(\sigma, \phi_0, T)] = \frac{4eT}{\tau_\perp} \sum_{\omega} \langle F_{\omega}(\mathbf{k}) \rangle^2 > 0 \quad (70)$$

and

$$\lim_{\sigma \rightarrow \infty} \left[\frac{J_{c,ise}^J(\sigma, \phi_0, T)}{J_{c,ise}^J(\sigma, 0, T)} \right] = 1 \quad \text{for general-}s\text{-wave OP's,} \quad (71)$$

whereas

$$\lim_{\sigma \rightarrow \infty} [J_{c,ide}^J(\sigma, \phi_0, T)] = 0, \quad (72)$$

$$\frac{J_{c,ide}^J(\sigma, \pi/4, T)}{J_{c,ide}^J(\sigma, 0, T)} = 0 \quad (\forall \sigma), \quad (73)$$

and

$$\lim_{\sigma \rightarrow \infty} \left[\frac{J_{c,ide}^J(\sigma, \phi_0, T)}{J_{c,ide}^J(\sigma, 0, T)} \right] \approx |\cos(2\phi_0)|,$$

for general- $d_{x^2-y^2}$ -wave OP's. (74)

Equation (70) is the Ambegaokar-Baratoff result,²⁴ which holds for all general- s -wave OP's with a nonvanishing average over the Fermi surface. In Eq. (74), the relation is exact in all of the models we investigated, except for the exponential model, for which it is still a good approximation. Hence, the more incoherent the tunneling, the easier it is for the c -axis twist experiment to distinguish the OP's.

V. OTHER FEATURES OF INCOHERENT c -AXIS TUNNELING

Next, we studied the reductions in the product $I_c R_n$ of the critical current times the resistance across a junction from the AB limit, $I_c R_n(T)|_{AB}$, for the case of a fully extended- s -wave OP, defined in Eq. (23) with $\epsilon=0$, as $\sigma \rightarrow \infty$.²⁴ We first define

$$I_c R_n(T) = C(T/T_c) I_c R_n(T)|_{AB}, \quad (75)$$

where the AB limit curve corresponds to the ordinary- s -wave case with $\sigma \rightarrow \infty$ for any Fermi surface. A few limits can be investigated analytically. For a circular Fermi-surface cross section, we can analytically evaluate $I_c R_n$ for all five models both at T_c and as $T \rightarrow 0$. We find $C(1) = (2/\pi)^2 \approx 0.405$, as in Sec. III A, and $C(0) = (2/\pi)^2 \ln 4 \approx 0.562$.

For the Fermi surface shown in Fig. 1, we find numerically in the incoherent limit for all five tunneling models that $C(0.9) = 0.416$, $C(0.5) = 0.465$, and $C(0) = 0.572$. For the slightly different Fermi surface studied elsewhere,^{41,45} with $t'/t = 1.3$ and $\mu/t = -0.6$, we found $C(0.9) = 0.400$, $C(0.5) = 0.450$, and $C(0) = 0.578$. Thus, the result of Yurgens *et al.*

that $I_c R_n(T=0) \approx 10$ mV for the HgBr₂-intercalated Bi2212 is in rather good agreement with that expected for an extended-*s* OP.²¹

Although there have not yet been many infrared reflectance measurements on Bi2212, the available experiments strongly suggest that the *c*-axis tunneling is not metallic.⁵⁸ In Ref. 58, not only was no Drude edge above 30 cm⁻¹ seen in the *c*-axis conduction in the normal state, none was seen in the superconducting state as well. In addition, there is now strong evidence that all underdoped HTSC have incoherent *c*-axis normal-state tunneling, with the sole exception of YBCO with $\delta \leq 0.15$.^{59–62} This is also the case in the recent measurements on the electron-doped material NCCO.⁶³ Although above T_c , the nonmetallic behavior is clearly seen, below T_c , metalliclike behavior reminiscent of a Drude edge for wave vectors in the range 10–200 cm⁻¹ has been observed,⁶⁰ although none has yet been seen in Bi2212.⁵⁸ This metalliclike behavior is most likely associated with the *c*-axis supercurrent.⁶⁰ Thus, if Bi2212 were to behave the same as the other materials with an incoherent *c*-axis normal-state conduction, one would expect it to show this same metalliclike behavior below T_c .

There have been two other schools of thought on this issue. One is that the interlayer tunneling processes change dramatically from incoherent to coherent below T_c .⁶⁴ Our analysis of the *c*-axis twist experiments of Li *et al.* strongly contradicts this idea, since the quasiparticle tunneling below T_c must be strongly incoherent. The second school holds that there is no quasiparticle tunneling below T_c due to an “orthogonality catastrophe,” but that the only tunneling process occurs by the simultaneous tunneling of pairs.⁶⁵ However, the fact that HgBr₂-intercalated Bi2212 has nearly the same T_c as does unintercalated Bi2212 argues strongly that this interlayer pair tunneling model as a mechanism for superconductivity is not correct.²¹ Thus, we consider it much more likely that the superconductivity arises from intralayer pairing. Then the individual particles do the actual tunneling.

Another experimental observation relevant to the question of the *c*-axis tunneling coherence is the apparent violation of the conventional sum rule, as observed by Basov *et al.*⁶⁰ This was investigated theoretically by Kim and Carbotte (KC).⁵⁴ Those workers assumed a $d_{x^2-y^2}$ -wave OP, and an incoherent interlayer tunneling matrix element squared of the form $f^J(\phi_{\mathbf{k}}, \phi_{\mathbf{k}'}) = |V_0| + |V_1|^2 \cos(2\phi_{\mathbf{k}}) \cos(2\phi_{\mathbf{k}'})$. By equating $1/\lambda_c^2$ derived from the conductivity and the superfluid density ρ_S , each evaluated to lowest order in f^J , they wrote (without the $i\zeta\epsilon$ superscripts)⁵⁴

$$\delta N_{i\zeta\epsilon}(T/T_c) = \frac{1}{2} + \frac{\sum_{\omega} \langle f^J(\gamma, \phi_{\mathbf{k}}, \phi_{\mathbf{k}'}) [1 - \omega_{i\zeta\epsilon, \mathbf{k}} \omega_{i\zeta\epsilon, \mathbf{k}'}] \rangle}{2 \sum_{\omega} \langle f^J(\gamma, \phi_{\mathbf{k}}, \phi_{\mathbf{k}'}) \delta_{i\zeta\epsilon, \mathbf{k}} \delta_{i\zeta\epsilon, \mathbf{k}'} \rangle}, \quad (76)$$

where $\delta N_{i\zeta\epsilon} = (N_N - N_{S, i\zeta\epsilon}) / \rho_{S, i\zeta\epsilon}$, $\omega_{i\zeta\epsilon, \mathbf{k}} = \omega / \Omega_{i\zeta\epsilon, \mathbf{k}}$, $\omega_{i\zeta\epsilon, \mathbf{k}'} = \omega / \Omega_{i\zeta\epsilon, \mathbf{k}'}$, $\delta_{i\zeta\epsilon, \mathbf{k}} = \Delta_{i\zeta\epsilon}(\phi_{\mathbf{k}}, T) / \Omega_{i\zeta\epsilon, \mathbf{k}}$, $\delta_{i\zeta\epsilon, \mathbf{k}'} = \Delta_{i\zeta\epsilon}(\phi_{\mathbf{k}'}, T) / \Omega_{i\zeta\epsilon, \mathbf{k}'}$, $\Omega_{i\zeta\epsilon, \mathbf{k}} = [\omega^2 + \Delta_{i\zeta\epsilon}^2(\phi_{\mathbf{k}}, T)]^{1/2}$, and $\Omega_{i\zeta\epsilon, \mathbf{k}'} = [\omega^2 + \Delta_{i\zeta\epsilon}^2(\phi_{\mathbf{k}'}, T)]^{1/2}$. It is easy to show that for

coherent tunneling with a rotationally-invariant f^J , $\delta N_{i\zeta\epsilon}(T/T_c) = 1$ for any OP, for all $T/T_c \leq 1$, and that $\delta N_{os}(T/T_c) = 1$, regardless of the form of $f^J(\phi_{\mathbf{k}}, \phi_{\mathbf{k}'})$. For the $d_{x^2-y^2}$ -wave case, KC showed that incoherent tunneling gives a conductivity sum-rule violation that is strong and of the wrong sign.^{54,60,66} They gave a lower limit on the violation, based upon restrictions of the parameters V_0 and V_1 . However, KC did not calculate the sum-rule violation resulting from other OP forms.

We studied this effect in our five circular Fermi-surface tunneling models. In most of these models, we can analytically perform the calculations at T_c for the $i = o, e, c, a$, $\zeta = s, d$ cases, corresponding to the notation in Eqs. (22)–(29). We shall first present the exact formulas for general-*s*- and $d_{x^2-y^2}$ -wave OP forms, both for the rotationally invariant tunneling models, and for the Lorentzian model, evaluated at T_c . The general formulas for the $\delta N_{i\zeta\epsilon}(1)$ for the rotationally invariant and the Lorentzian tunneling models are given in Appendix D.

We first consider the coherent limit. In this limit, each of the $f_{4n}(\gamma)$ and $f_{4n+2}(\gamma)$ approach unity. Thus, from Eqs. (D1) and (D2) in Appendix D, all of the rotationally invariant tunneling models show no sum-rule violation for any of the OP models in the coherent limit. For the Lorentzian tunneling model, our results are given in Eqs. (D3) and (D4) in Appendix D. We note from Eq. (B19) that $f_{n,m}^L(\gamma \rightarrow \infty)$ is only a function of m . Thus, it is also easy to see that both the general-*s*- and $d_{x^2-y^2}$ -wave OP forms satisfy the sum rule even for the nonrotationally invariant Lorentzian tunneling model. This is interesting because the Lorentzian model gives rise to slightly larger critical current values for each of the anisotropic OP's than do the other models.

We now discuss the particular OP and tunneling models away from the coherent limit. In the incoherent limit for a general-*s*-wave OP, all five of the tunneling models reduce to the sum-rule violation amount

$$\delta N_{is\epsilon}(1) - 1 \rightarrow \frac{\sum_{n=1}^{\infty} a_{isn}^2(\epsilon)}{4a_{is0}^2(\epsilon)}. \quad (77)$$

Clearly, the ordinary-*s*-wave OP gives $\delta N_{os}(1) - 1 = 0$. From Eqs. (A3), (A4), and (33), we find as $\gamma \rightarrow 0$,

$$\delta N_{es0}(1) - 1 = \delta N_{cs0}(1) - 1 \rightarrow \sum_{n=1}^{\infty} \frac{1}{[(2n)^2 - 1]^2} \approx 0.117, \quad (78)$$

$$\delta N_{as\epsilon}(1) - 1 \rightarrow \frac{1}{4\epsilon^2 + c_a(\epsilon, \gamma)}, \quad (79)$$

where $c_a(\epsilon, 0)$ vanishes as $\gamma \rightarrow 0$ if $\epsilon \neq 0$. Thus, the extended- and compressed-*s*-wave OP's only violate the sum rule by a small amount, albeit of the wrong sign. The anomalous-*s*-wave OP, on the other hand, violates the sum rule by a large amount, especially if $\epsilon \ll 1$. In this case, we expand $c_a(\epsilon, \gamma)$ for both $\epsilon \ll 1$ and $\gamma \ll 1$. We find $c_a(\epsilon, \gamma) \rightarrow (\gamma/2)^4$ in the rotationally invariant and stretched Lorentzian models,

$(\gamma/2)^4/(4!)$ in the Gaussian model, $4(2\gamma)^{1/2}/(63\pi)$ in the exponential model, and $\epsilon\gamma^2+383\gamma^4/128$ in the Lorentzian model. Thus, for $\epsilon=0$, these functions all diverge as $\gamma\rightarrow 0$, with the exponential model giving the slowest divergence.

For the general- $d_{x^2-y^2}$ -wave models in the incoherent limit, the Gaussian, Lorentzian, rotationally invariant Lorentzian, and stretched Lorentzian tunneling models all behave similarly, yielding

$$\delta N_{id\epsilon}(1) - \frac{1}{2} \rightarrow \frac{\sum_{n=0}^{\infty} a_{idn}^2(\epsilon)}{2a_{id0}^2(\epsilon)c_d\gamma^2}, \quad (80)$$

where $c_d = \frac{1}{8}$ in the Gaussian model, $\frac{13}{8}$ in the Lorentzian model, $-\frac{1}{4}$ in the rotationally invariant model, and $\frac{1}{4}$ in the stretched Lorentzian model. The negative sign obtained for all of the $d_{x^2-y^2}$ -wave OP's in the rotationally invariant model has an origin that is similar to the change in sign obtained in the critical current. The OP forms give rise to the overall factors $C_{id}(\epsilon) = \sum_{n=0}^{\infty} a_{idn}^2(\epsilon)/a_{id0}^2(\epsilon)$ for $i = o, e, c, a$. We find $C_{od} = 1$, $C_{ed}(0) = 1 + 9\sum_{n=1}^{\infty} [(2n+3) \times (2n+1)(2n-1)]^{-2} \approx 1.041$, $C_{cd}(0) = 1 + 9\sum_{n=1}^{\infty} [(2n+3)(2n-1)]^{-2} \approx 1.39$, and $C_{ad}(\epsilon) = 1 + 1/(2\epsilon+1)^2$. Except for the rotationally invariant Lorentzian tunneling model, the sum-rule violation is strong and of the opposite sign to that observed in experiment for all of these $d_{x^2-y^2}$ -wave OP's, but the OP ranking in terms of increased sum-rule violation is ordinary-, extended-, compressed-, and anomalous- $d_{x^2-y^2}$ wave, respectively.

For the exponential tunneling model, the situation is a bit more complicated. Near the incoherent limit, we obtain for the $d_{x^2-y^2}$ -wave functions,

$$\delta N_{id\epsilon}(1) - \frac{1}{2} \rightarrow \frac{\pi \sum_{n=0}^{\infty} a_{idn}^2(\epsilon)}{4(2\gamma)^{1/2} \sum_{n=0}^{\infty} a_{idn}^2(\epsilon) / [(8n+4)^2 - 1]}, \quad (81)$$

which diverges only as $\gamma^{-1/2}$ instead of γ^{-2} for the other models, but it also depends slightly more on the particular OP form than do the results for other tunneling models. Letting $\delta N_{id\epsilon}(1) - \frac{1}{2} = 15\pi C_{id}^E(\epsilon)/[4(2\gamma)^{1/2}]$, we find $C_{od}^E = 1$, $C_{ed}^E(0) \approx 1.04$, $C_{cd}^E(0) \approx 1.38$, and $C_{ad}^E(\epsilon) = [(2\epsilon+1)^2 + 1]/[(2\epsilon+1)^2 + \frac{15}{143}]$. The OP ranking in terms of the violation of the sum rule is thus the same as for the Gaussian, Lorentzian, and stretched Lorentzian tunneling models.

For the extended- and compressed- s -wave OP's in the incoherent limit of all five tunneling models, $\delta N_{is\epsilon}(1) \rightarrow 1/2 + (1+2\epsilon^2)/\{(1+\epsilon^2)[4E(k)/\pi]^2\}$, which varies between a maximum of ≈ 1.117 as $\epsilon \rightarrow 0$ and 1 as $\epsilon \rightarrow \infty$. At the intermediate value $\epsilon = 1$, $\delta N_{is1}(1) \approx 1.007$. As $T \rightarrow 0$ in the coherent limit $\gamma \rightarrow \infty$, we again have $\delta N_{\zeta}(0) = 1$ in the four rotationally invariant tunneling models for all OP's, as expected. As $T \rightarrow 0$ in the incoherent limit for both $\zeta = cs, es$, we can evaluate the denominator in Eq. (76) exactly in all five tunneling models, and the numerator numerically. We

find $\delta N_{es0}(0) = \delta N_{cs0}(0) \rightarrow 1.087$. All of the $d_{x^2-y^2}$ -wave OP's have divergent $\delta N_{id\epsilon}(0)$ values.

We thus conclude that none of the eight OP's gives a $\delta N < 1$ in most tunneling models. However, near the incoherent limit, the four $d_{x^2-y^2}$ -wave cases and the fully anomalous- s -wave case are by far the worst, except for the rotationally invariant Lorentzian model. In that case, each of the $d_{x^2-y^2}$ -wave OP's gave rise to a sum-rule violation that was both large and of the same sign as observed in experiment.⁶⁰ Except for this particular case, it is likely to be much easier to construct a theory that can incorporate both incoherent interlayer tunneling and a $\delta N < 1$ if the OP is a general- s -wave one, and not a $d_{x^2-y^2}$ -wave one. But even for an s -wave OP that changes sign on the Fermi surface, such as the anomalous- s -wave OP, these results make a reconciliation with the sum-rule violation more difficult.

VI. SUMMARY AND CONCLUSIONS

An important question to resolve is the amount of coherence of the tunneling processes. Since coherent tunneling preserves the momentum parallel to the junction, and incoherent tunneling allows a random change in parallel momentum, it is important to determine just how sensitive the intermediate coherence regime is to the particular form of the tunneling matrix element squared. We have therefore studied five models of Josephson tunnel junctions, which are designed to be applicable to the high-temperature superconductor materials. In particular, these models are, respectively, Gaussian, exponential, Lorentzian, and two versions of Lorentzian, which we denote rotationally invariant Lorentzian and stretched Lorentzian. These models interpolate smoothly between the coherent and incoherent tunneling limits by varying a single parameter.

An experiment that can provide information about the amount of coherence in the intrinsic c -axis tunneling in Bi2212 is the bicrystal c -axis twist junction experiment.⁸ Since Bi2212 is generally thought to have a Fermi surface that is not rotationally invariant about the Γ point,^{42,43} rotating one layer with respect to an adjacent one about the c axis forces the quasiparticles to either change momentum or energy during the tunneling process. Thus, to emphasize the differences between different Fermi surfaces we have studied two model Fermi surfaces, one which is circular and centered about the Γ point, and the other which has been specifically chosen to fit the Bi2212 Fermi surface as measured in angle-resolved photoemission spectroscopy experiments.⁴³

In addition, an important study that can also be made is to test the orbital symmetry of the OP. When the superconducting layers are very weakly coupled, the OP must lock onto the lattice on each layer.⁴⁰ Thus, OP's on opposite sides of the twist junction will be rotated with respect to one another. In coherent tunneling through a twist junction, a particle will be transferred to a different energy state, if the OP is in any way anisotropic. Since the particular crystal structure of Bi2212 allows the OP to be in one of only two groups, one containing all functions with s -wave symmetry and the other containing all functions of $d_{x^2-y^2}$ -wave symmetry,⁴⁰ we have modeled each of these general OP symmetries with four

simple OP forms. The s -wave OP's are a constant, an extended- s -wave OP, which has nodes along the Γ - X and Γ - Y lines, but which does not change sign on the Fermi surface, a compressed- s -wave OP, which has nodes at the points at which the Bi2212 Fermi surface intersects the Brillouin-zone edge, and an anomalous- s -wave OP, which arises from near-neighbor attractive pairing. This OP has nodes on the Fermi surface at points different from the extended- s and compressed- s -wave OP's, and changes sign on the Fermi surface, averaging to zero in the entire Brillouin zone, but not on the Fermi surface.

We first proved a theorem, which states that for weak, time-reversal-invariant tunneling between layers of a tetragonal crystal twisted 45° about the c axis with respect to one another, the c -axis critical current for a superconductor with either general- $d_{x^2-y^2}$ - or general- d_{xy} -wave symmetry vanishes. Since the three exceptional cases to these requirements, slight orthorhombicity, mixing of $d_{x^2-y^2}$ and d_{xy} or other OP components, and higher-order (strong) tunneling processes, have already been discussed in the literature^{40,41} and found to be unable to explain the experiments with a dominant $d_{x^2-y^2}$ -wave OP, it is important to show just how robust is the interpretation of the experimental results. The result that the critical current density across the twist junction is the same as that across the single crystal itself is profound.⁸ First, it implies that the tunneling must be very incoherent. In order to fit the data with models that have rather sharp cutoffs in the parallel momentum change, such as the Gaussian model, it is necessary for the change in quasiparticle momentum to cover roughly 30% of the Brillouin zone. If one were to identify the full width at half maximum (FWHM) in the tunneling amplitude as a cutoff for the other models we studied, this would reduce to only $\approx 7\%$ of the BZ. However, such models allow a substantial number of processes well beyond the FWHM.

In any event, there is also one other inescapable conclusion of the experiment. We showed for quite general tunneling forms near to the incoherent limit that the differences between the twist angle dependence of the Josephson tunneling between an s -wave and a $d_{x^2-y^2}$ -wave superconductor become the most robust. In this limit, $J_{c,s}(\phi_0, T)/J_{c,s}(0, T) = 1$ for $T \leq T_c$, but for the $d_{x^2-y^2}$ -wave case, $J_{c,d}(\phi_0, T) = 0$, and the ratio of the two vanishing quantities $J_{c,d}(\phi_0, T)/J_{c,d}(0, T) \approx |\cos(2\phi_0)|$, for $T \leq T_c$. In addition, we showed by studying five specific tunneling models and four varieties of $d_{x^2-y^2}$ -wave OP forms that none of the d -wave OP forms could fit the data. However, each of the four general- s -wave OP forms we studied can easily fit the data, provided that the tunneling is very incoherent. Thus, we conclude that the OP on each side of the junction cannot possibly be of pure $d_{x^2-y^2}$ -wave symmetry. This conclusion also must apply to the untwisted intrinsic junctions in the bulk of the Bi2212 single crystal.

In addition, we applied our models for the circular Fermi surface (at $\phi_0 = 0$) to investigate the question of how the degree of coherence affects the Thomas-Reiche-Kuhn sum-rule violation in c -axis transport. We used the simple approach of Kim and Carbotte,⁵⁴ and found that none of the s -wave OP's we studied can give rise to a sum-rule violation

of the sign that has been observed in optical reflectivity experiments. Except for the anomalous- s -wave OP, the sum-rule violation was rather small. For the $d_{x^2-y^2}$ -wave OP's, the sign of the sum-rule violation depends upon the details of the tunneling model. For most models, the sign is opposite to that which has been observed, and the magnitude is very large. However, for the sufficiently incoherent rotationally invariant Lorentzian tunneling model, each of the $d_{x^2-y^2}$ -wave OP's studied has a large sum-rule violation of the same sign that was observed. In this particular case, the untwisted junctions appear to act like π junctions.

In conclusion, we found that the c -axis twist experiments of Li *et al.* provide compelling evidence that the c -axis tunneling in Bi2212 is strongly incoherent.⁸ As a consequence, the experiment cannot distinguish between an isotropic s -wave and an extremely anisotropic s -wave OP. However, the purported $d_{x^2-y^2}$ -wave OP is inconsistent with the experiments. These conclusions appear to be incompatible with those derived from the tricrystal experiment.¹

There are only two possible scenarios that might allow for a compatibility. One is that the s - and $d_{x^2-y^2}$ -wave OP's have indistinguishable T_c values. However, since T_c depends upon doping and impurities, it is unlikely that this will be the case in every sample studied. Second, it is possible that the mirror plane symmetry (the bc plane containing the periodic lattice distortion) we and others have generally assumed to be present in Bi2212 could be broken. One electron-diffraction experiment performed long ago on a different Bi2212 sample is suggestive of this scenario.⁶⁷ But, explicit electron-diffraction studies of the samples used by Li *et al.* indicate that 90% of them do exhibit the bc -mirror plane.⁶⁸ Experiments to test this hypothesis are currently planned. Since neither the c -axis twist experiment nor the tricrystal experiment has yet been fully reproduced in a second laboratory, it remains to be seen which will ultimately prevail. We encourage reproduction of the c -axis twist experiment using mesa structures, so that the currents can be safely assumed to be uniform over the entire junctions, both I_c and R_n can be measured, and the Fraunhofer pattern can be obtained.

ACKNOWLEDGMENTS

The authors thank G. Arnold, R. Kleiner, A. J. Leggett, Qiang Li, and M. Möhle for useful discussions. One of us (R.A.K.) would like to thank T. Hasegawa for partial support and for showing him directly a few of the problems with SQUID microscope flux integrations. This work was supported by U.S. D.O.E.-BES Contract No. W-31-109-ENG-38, NATO Collaborative Research Grant No. 960102, the U.S. Office of Naval Research Contract No. N00014-94-1-0147, and by the DFG through the Graduiertenkolleg "Physik nanostrukturierter Festkörper."

APPENDIX A

The coefficients of the real-space expansion of the extended and compressed OP's in Eqs. (16) and (17) are easily obtained in the limit $\epsilon \rightarrow 0$ by Fourier series transformation. For $i = e, c$, these are

$$a_{e,nm}(0) = \frac{8}{\pi^2} \frac{(2 - \delta_{n,0})(2 - \delta_{m,0})}{[(n-m)^2 - 1][(n+m)^2 - 1]}, \quad (\text{A1})$$

$$a_{c,nm}(0) = \frac{4}{\pi^2} \frac{(2 - \delta_{n,0})(2 - \delta_{m,0})}{[(2n)^2 - 1][(2m)^2 - 1]}. \quad (\text{A2})$$

For the circular Fermi-surface model, the analogous coefficients of the extended and compressed OP's in Eqs. (30) and (31) are

$$a_{esn}(0) = \frac{2(-1)^{n+1}(2 - \delta_{n,0})}{\pi[(2n)^2 - 1]}, \quad (\text{A3})$$

$$a_{csn}(0) = \frac{-2(2 - \delta_{n,0})}{\pi[(2n)^2 - 1]}, \quad (\text{A4})$$

$$a_{edn}(0) = \frac{8(-1)^{n+1}}{\pi(2n+3)(2n+1)(2n-1)}, \quad (\text{A5})$$

and

$$a_{cdn}(0) = \frac{-4}{\pi(2n+3)(2n-1)}. \quad (\text{A6})$$

APPENDIX B

For the four specific rotationally invariant tunneling models, Eqs. (42), (43), (45), and (46), the respective $f_n(\gamma)$ values obtained from Eq. (51) are

$$f_{nG}(\gamma) = I_n(\gamma)/I_0(\gamma), \quad (\text{B1})$$

$$f_{nE}(\gamma) = \frac{\int_0^\pi dx \exp[-(2\gamma)^{1/2} \sin x] \cos(2nx)}{\int_0^\pi dx \exp[-(2\gamma)^{1/2} \sin x]}, \quad (\text{B2})$$

$f_{nRL}(\gamma)$

$$= \text{Re} \left(\frac{[1 - i/\gamma + i(1 + 2i\gamma)^{1/2}/\gamma]^n}{(1 + 2i\gamma)^{1/2}} \right) / \text{Re} \frac{1}{(1 + 2i\gamma)^{1/2}}, \quad (\text{B3})$$

and

$$f_{nSL}(\gamma) = \left[\frac{\gamma}{1 + \gamma + (1 + 2\gamma)^{1/2}} \right]^n. \quad (\text{B4})$$

Asymptotically, these functions approach the coherent limit $\gamma \rightarrow \infty$ as

$$f_{nG}(\gamma) \rightarrow 1 - \frac{n^2}{2\gamma}, \quad (\text{B5})$$

$$f_{nE}(\gamma) \rightarrow 1 - \frac{2n^2}{\gamma}, \quad (\text{B6})$$

$$f_{nRL}(\gamma) \rightarrow 1 - \frac{n^2}{\gamma}, \quad (\text{B7})$$

and

$$f_{nSL}(\gamma) \rightarrow 1 - \frac{2^{1/2}n}{\gamma^{1/2}}. \quad (\text{B8})$$

They approach the incoherent limit $\gamma \rightarrow 0$ as

$$f_{nG}(\gamma) \rightarrow \frac{(-\gamma/2)^n}{n!}, \quad (\text{B9})$$

$$f_{nE}(\gamma) \rightarrow \delta_{n,0} + (1 - \delta_{n,0}) \frac{2(2\gamma)^{1/2}}{\pi[(2n)^2 - 1]}, \quad (\text{B10})$$

$$f_{nRL}(\gamma) \rightarrow \begin{cases} (-1)^m (\gamma/2)^{2m} & : n = 2m, \\ (-1)^m \gamma^{2m+2} (m+1)/2^{2m} & : n = 2m+1, \end{cases} \quad (\text{B11})$$

and

$$f_{nSL} \rightarrow (\gamma/2)^n. \quad (\text{B12})$$

For the Lorentzian model, the $f_{n,m}^L(\gamma)$ in Eq. (52) are defined by

$$f_{n,m}^L(\gamma) = \frac{1}{D_0} \int_0^\pi \frac{d\phi x^{2m}(\phi) \cos(2n\phi)}{\pi 2^m D_1[x(\phi)] D_2^m[x(\phi)]}, \quad (\text{B13})$$

$$x(\phi) = \gamma(1 - \cos 2\phi), \quad (\text{B14})$$

$$D_1(x) = (1+x)(1+2x)^{1/2}, \quad (\text{B15})$$

$$D_2(x) = 1 + 2x + x^2/2 + (1+x)(1+2x)^{1/2}, \quad (\text{B16})$$

and

$$D_0 = \int_0^{\pi/2} \frac{2d\phi}{\pi D_1[x(\phi)]}. \quad (\text{B17})$$

In the coherent limit $\gamma \rightarrow \infty$, the $f_{n,m}^L(\gamma)$ approach

$$f_{n,m}^L(\gamma) \rightarrow C_m^L - \mathcal{O}\left(\frac{\ln \gamma}{\gamma}\right), \quad (\text{B18})$$

where

$$C_m^L = \int_0^\infty \frac{dx \tanh^{4m}(x/2)}{1 + \cosh^2 x} / \int_0^\infty \frac{dx}{1 + \cosh^2 x}. \quad (\text{B19})$$

As $\gamma \rightarrow 0$, the leading γ dependencies of the $f_{n,m}^L(\gamma)$ for the lowest even n values are

$$f_{0,m}^L(\gamma) \rightarrow \frac{\gamma^{2m}}{2^{3m}} \binom{4m}{2m}, \quad (\text{B20})$$

$$f_{2,m}^L(\gamma) \rightarrow \frac{7}{8} \gamma^2 \delta_{m,0} + \frac{\gamma^{2m} \Theta(m-1)}{2^{3m}} \binom{4m}{2m-2}, \quad (\text{B21})$$

$$f_{4,m}^L(\gamma) \rightarrow \frac{\gamma^4}{2^7} (83\delta_{m,0} + 14\delta_{m,1}) + \frac{\gamma^{2m} \Theta(m-2)}{2^{3m}} \binom{4m}{2m-4}, \quad (\text{B22})$$

$$f_{6,m}^L(\gamma) \rightarrow \frac{\gamma^6}{2^{10}}(543\delta_{m,0} + 83\delta_{m,1} + 14\delta_{m,2}) + \frac{\gamma^{2m}\Theta(m-3)}{2^{3m}} \binom{4m}{2m-6}, \quad (\text{B23})$$

etc., where $\Theta(n) = 1$ for $n \geq 0$, and $\Theta(n) = 0$ for $n < 0$ is the Heaviside step function. In particular, $f_{od}(\gamma, 0)$ in the Lorentzian model approaches the incoherent limit $\gamma \rightarrow 0$ as $\frac{13}{16}\gamma^2$.

APPENDIX C

Here we present the details of the expansion of a rotation-

ally invariant tunneling matrix element squared in powers of $\mathbf{k} \cdot \mathbf{k}'$. First, we note that $A_{l\mu}$ can be written as

$$A_{l\mu} = \delta_{l,0} + (1 - \delta_{l,0}) \frac{1}{(2l)!} \prod_{p=0}^{2l-1} (\mu/2 - p). \quad (\text{C1})$$

For $\mu = 2$, only the $l = 0, 1$ terms remain. For $\mu = 2q$, an even integer, the $A_{l\mu} = 0$ for $l \geq q$. For $0 < \mu < 2$, all of the $A_{l\mu} < 0$, except for $A_{0\mu}$.

We begin by using polar coordinates, obtaining

$$(2\tilde{\mathbf{k}} \cdot \tilde{\mathbf{k}}')^{2l} = (2kk')^{2l} \cos^{2l}(\phi_{\mathbf{k}} - \phi_{\mathbf{k}'} - \phi_0) \quad (\text{C2})$$

$$= (kk')^{2l} \sum_{p=0}^l (2 - \delta_{p,0}) \cos[2p(\phi_{\mathbf{k}} - \phi_{\mathbf{k}'} - \phi_0)] \binom{2l}{l+p} \quad (\text{C3})$$

$$\begin{aligned} &= \sum_{m=0}^{E(\frac{l}{2})} C_{slm} \left(\cos(4m\phi_0) [S^{lm}(\mathbf{k})S^{lm}(\mathbf{k}') + G_{xy(x^2-y^2)}^{lm}(\mathbf{k})G_{xy(x^2-y^2)}^{lm}(\mathbf{k}')] + \sin(4m\phi_0) [G_{xy(x^2-y^2)}^{lm}(\mathbf{k})S^{lm}(\mathbf{k}') \right. \\ &\quad \left. - S^{lm}(\mathbf{k})G_{xy(x^2-y^2)}^{lm}(\mathbf{k}')] \right) + \sum_{m=0}^{E(\frac{l-1}{2})} C_{dlm} \left(\cos[(4m+2)\phi_0] [D_{x^2-y^2}^{lm}(\mathbf{k})D_{x^2-y^2}^{lm}(\mathbf{k}') + D_{xy}^{lm}(\mathbf{k})D_{xy}^{lm}(\mathbf{k}')] \right. \\ &\quad \left. + \sin[(4m+2)\phi_0] [D_{xy}^{lm}(\mathbf{k})D_{x^2-y^2}^{lm}(\mathbf{k}') - D_{x^2-y^2}^{lm}(\mathbf{k})D_{xy}^{lm}(\mathbf{k}')] \right), \quad (\text{C4}) \end{aligned}$$

where

$$C_{slm} = (2 - \delta_{m,0}) \binom{2l}{l+2m}, \quad (\text{C5})$$

$$C_{dlm} = 2 \binom{2l}{l+2m+1}, \quad (\text{C6})$$

and $E(x)$ is the largest nonnegative integer $\leq x$. In polar coordinates, the tunnel functions are given by

$$S^{lm}(\mathbf{k}) = k^{2l} \cos(4m\phi_{\mathbf{k}}) \quad \text{for } 0 \leq m \leq E\left(\frac{l}{2}\right), \quad (\text{C7})$$

TABLE I. Tunnel functions in rectangular coordinates for $l \leq 4$.

| (lm) | $S^{lm}(\mathbf{k})$ | $G_{xy(x^2-y^2)}^{lm}(\mathbf{k})$ | $D_{x^2-y^2}^{lm}(\mathbf{k})$ | $D_{xy}^{lm}(\mathbf{k})$ |
|--------|--|--|--|---|
| (00) | 1 | 0 | 0 | 0 |
| (10) | k^2 | 0 | $k_x^2 - k_y^2$ | $2k_x k_y$ |
| (20) | k^4 | 0 | $(k_x^2 - k_y^2)^2$ | $2k_x k_y k^2$ |
| (21) | $k^4 - 8k_x^2 k_y^2$ | $2k_x k_y (k_x^2 - k_y^2)$ | 0 | 0 |
| (30) | k^6 | 0 | $(k_x^2 - k_y^2)^4$ | $2k_x k_y k^4$ |
| (31) | $(k^4 - 8k_x^2 k_y^2) k^2$ | $2k_x k_y (k_x^2 k_y^2) k^2$ | $[(k_x^2 - k_y^2) \times (k^4 - 16k_x^2 k_y^2)]$ | $[2k_x k_y \times (k^4 - 16k_x^2 k_y^2)]$ |
| (40) | k^8 | 0 | $(k_x^2 - k_y^2)^6$ | $2k_x k_y k^6$ |
| (41) | $(k^4 - 8k_x^2 k_y^2) k^4$ | $2k_x k_y (k_x^2 - k_y^2) k^4$ | $[(k_x^2 - k_y^2)^2 \times (k^4 - 16k_x^2 k_y^2)]$ | $[2k_x k_y k^2 \times (k^4 - 16k_x^2 k_y^2)]$ |
| (42) | $[k^8 - 32k_x^4 k_y^2 k_y^2 + 128k_x^4 k_y^4]$ | $[4k_x k_y (k_x^2 - k_y^2) \times (k^4 - 8k_x^2 k_y^2)]$ | 0 | 0 |

$$D_{x^2-y^2}^{lm}(\mathbf{k}) = k^{2l} \cos[(4m+2)\phi_{\mathbf{k}}] \quad \text{for } 0 \leq m \leq E\left(\frac{l-1}{2}\right), \quad (\text{C8})$$

$$D_{xy}^{lm}(\mathbf{k}) = k^{2l} \sin[(4m+2)\phi_{\mathbf{k}}] \quad \text{for } 0 \leq m \leq D\left(\frac{l-1}{2}\right), \quad (\text{C9})$$

and

$$G_{xy(x^2-y^2)}^{lm}(\mathbf{k}) = k^{2l} \sin(4m\phi_{\mathbf{k}}) \quad \text{for } 1 \leq m \leq E\left(\frac{l}{2}\right). \quad (\text{C10})$$

These functions are elements of the general- s -, $d_{x^2-y^2}$ -, d_{xy} -, and $g_{xy(x^2-y^2)}$ -wave-function sets, respectively. Elements of different function sets are orthogonal with each other when integrated over $\phi_{\mathbf{k}}$ at fixed k ,

$$\int_0^{2\pi} d\phi_{\mathbf{k}} S^{lm}(\mathbf{k}) D_{x^2-y^2}^{l'm'}(\mathbf{k}) = 0, \quad (\text{C11})$$

etc. We also have that elements from the same function set with different m values are orthogonal when integrated over $\phi_{\mathbf{k}}$ at fixed k ,

$$\int_0^{2\pi} d\phi_{\mathbf{k}} S^{lm}(\mathbf{k}) S^{l'm'}(\mathbf{k}) = \pi k^{2(l+l')} \delta_{m,m'} (1 + \delta_{m,0}), \quad (\text{C12})$$

and similar relations for elements of the other function sets.

In Table I, we present the tunnel functions for $l \leq 4$ in rectangular coordinates. In this representation, elements from different function sets are orthogonal over the first BZ and over a Fermi surface of tetragonal symmetry,

$$\int_{-\pi/a}^{\pi/a} dk_x \int_{-\pi/a}^{\pi/a} dk_y S^{lm}(\mathbf{k}) D_{x^2-y^2}^{l'm'}(\mathbf{k}) = 0, \quad (\text{C13})$$

etc., but elements within a function set with different (l, m) values are not orthogonal with each other on that domain.

APPENDIX D

Here we list the results for the sum-rule violation calculation. For the four rotationally invariant tunneling models, we obtain

$$\delta N_{is\epsilon}(1) = \frac{1}{2} \left(1 + \frac{\sum_{n=0}^{\infty} (1 + \delta_{n,0}) a_{isn}^2(\epsilon)}{\sum_{n=0}^{\infty} (1 + \delta_{n,0}) a_{isn}^2(\epsilon) f_{4n}(\gamma)} \right), \quad (\text{D1})$$

$$\delta N_{id\epsilon}(1) = \frac{1}{2} \left(1 + \frac{\sum_{n=0}^{\infty} a_{idn}^2(\epsilon)}{\sum_{n=0}^{\infty} a_{idn}^2(\epsilon) f_{4n+2}(\gamma)} \right), \quad (\text{D2})$$

where the $f_n(\gamma)$ are defined in Eq. (51). For the Lorentzian model, we find

$$\delta N_{is\epsilon}^L(1) = \frac{1}{2} \left(1 + \frac{\sum_{n,m=0}^{\infty} a_{isn}(\epsilon) a_{ism}(\epsilon) [f_{2n+2m,n+m}^L(\gamma) + f_{2|n-m|,|n-m|}^L(\gamma)]}{\sum_{n,m=0}^{\infty} a_{isn}(\epsilon) a_{ism}(\epsilon) [f_{2|n-m|,n+m}^L(\gamma) + f_{2n+2m,|n-m|}^L(\gamma)]} \right), \quad (\text{D3})$$

$$\delta N_{id\epsilon}^L(1) = \frac{1}{2} \left(1 + \frac{\sum_{n,m=0}^{\infty} a_{idn}(\epsilon) a_{idm}(\epsilon) [f_{2(n+m+1),n+m+1}^L(\gamma) + f_{2|n-m|,|n-m|}^L(\gamma)]}{\sum_{n,m=0}^{\infty} a_{idn}(\epsilon) a_{idm}(\epsilon) [f_{2|n-m|,n+m+1}^L(\gamma) + f_{2(n+m+1),|n-m|}^L(\gamma)]} \right), \quad (\text{D4})$$

where the $f_{n,m}^L(\gamma)$ are given in Eq. (B13).

*Present address: Max-Planck-Institut für Physik komplexer Systeme, Nöthnitzer Strasse 38, D-01187, Dresden, Germany. Email address: rklemm@mpipks-dresden.mpg.de

¹C.C. Tsuei, J.R. Kirtley, Z.F. Ren, J.H. Wang, H. Raffy, and Z.Z. Li, *Nature (London)* **387**, 481 (1997); J.R. Kirtley and C.C. Tsuei, *Rev. Mod. Phys.* **72**, 969 (2000).

²R.R. Schulz, B. Chesca, B. Goetz, C.W. Schneider, A. Schmehl, H. Bielefeldt, H. Hilgenkamp, J. Mannhart, and C.C. Tsuei, *Appl. Phys. Lett.* **76**, 912 (2000).

³C.C. Tsuei and J.R. Kirtley, *Phys. Rev. Lett.* **85**, 182 (2000).

⁴R. Prozorov, R.W. Gianetta, P. Fournier, and R.L. Greene, *Phys. Rev. Lett.* **85**, 3700 (2000).

⁵L. Alff, S. Meyer, S. Kleefisch, U. Schoop, A. Marx, H. Sato, M. Naito, and R. Gross, *Phys. Rev. Lett.* **83**, 2644 (1999); L. Alff, A. Beck, R. Gross, A. Marx, S. Kleefisch, T. Bauch, H. Saito, M. Naito, and G. Koren, *Phys. Rev. B* **58**, 11 197 (1998); S. Kleefisch, B. Welter, M. Naito, A. Marx, L. Alff, and R. Gross, *cond-mat/0101433* (unpublished).

⁶R. Krupke and G. Deutscher, *J. Low Temp. Phys.* **117**, 533 (1999).

⁷A. Bhattacharya, I. Zutic, O.T. Valls, A.M. Goldman, U. Welp, and B. Veal, *Phys. Rev. Lett.* **82**, 3132 (1999).

⁸Q. Li, Y.N. Tsay, M. Suenaga, R.A. Klemm, G.D. Gu, and N. Koshizuka, *Phys. Rev. Lett.* **83**, 4160 (1999).

⁹M. Möbke and R. Kleiner, *Phys. Rev. B* **59**, 4486 (1999).

¹⁰T. Kawayama, M. Kanai, T. Kawai, M. Maruyama, A. Fujimaki, and H. Hayakawa, *Physica C* **325**, 49 (1999).

¹¹S.I. Woods, A.S. Katz, T.L. Kirk, M.C. de Andrade, M.B. Maple, and R.C. Dynes, *IEEE Trans. Appl. Supercond.* **9**, 3917 (1999).

¹²D.A. Wollman, D.J. Van Harlingen, W.C. Lee, D.M. Ginsberg, and A. Leggett, *Phys. Rev. Lett.* **71**, 2134 (1993).

¹³D.A. Brawner and H.R. Ott, *Phys. Rev. B* **50**, 6530 (1994).

¹⁴Anna Mathai, Ph.D. thesis, University of Maryland, 1995.

¹⁵D.A. Wollman, D.J. Van Harlingen, J. Gianpintzakakis, and D.M. Ginsberg, *Phys. Rev. Lett.* **74**, 797 (1995).

¹⁶R. A. Klemm, in *Symmetry and Pairing in Superconductors*, ed-

- ited by M. Ausloos and S. Kruchinin (Kluwer, Dordrecht, 1999), pp. 161–172.
- ¹⁷K.A. Moler, J.R. Kirtley, D.G. Hinks, T.W. Li, and M. Xu, *Science* **279**, 1193 (1998).
- ¹⁸O.B. Hyun, J.R. Clem, and D.K. Finnemore, *Phys. Rev. B* **40**, 175 (1989).
- ¹⁹A. Mathai, Y. Gim, R.C. Black, A. Amar, and F.C. Wellstood, *Phys. Rev. Lett.* **74**, 4523 (1995).
- ²⁰Y. Gim, A. Mathai, R.C. Black, A. Amar, and F.C. Wellstood, *J. Phys. I* **6**, 2299 (1996); Yonggyu Gim, Ph.D. thesis, University of Maryland, 1996.
- ²¹A. Yurgens, D. Winkler, T. Claeson, S.-J. Hwang, and J.-H. Choy, *Int. J. Mod. Phys. B* **13**, 3758 (1999).
- ²²R. Kleiner, A.S. Katz, A.G. Sun, R. Summer, D.A. Gajewski, S.H. Han, S.I. Woods, E. Dantsker, B. Chen, K. Char, M.B. Maple, R.C. Dynes, and J. Clarke, *Phys. Rev. Lett.* **76**, 2161 (1996).
- ²³V.M. Krasnov, A. Yurgens, D. Winkler, P. Delsing, and T. Claeson, *Phys. Rev. Lett.* **84**, 5860 (2000); V.M. Krasnov, A.E. Kovalev, A. Yurgens, and D. Winkler, *ibid.* **86**, 2657 (2001).
- ²⁴V. Ambegaokar and A. Baratoff, *Phys. Rev. Lett.* **10**, 486 (1963); **11**, 104 (1963).
- ²⁵R.A. Klemm, G. Arnold, C.T. Rieck, and K. Scharnberg, *Phys. Rev. B* **58**, 14 203 (1998).
- ²⁶W. Braunisch, N. Knauf, G. Bauer, A. Kock, A. Becker, B. Freitag, A. Grütz, V. Kataev, S. Neuhausen, B. Ruden, D. Khomskii, D. Wohlleben, J. Bock, and E. Preisler, *Phys. Rev. B* **48**, 4030 (1993).
- ²⁷A.P. Nielsen, A.B. Cawthorne, P. Barbara, F.C. Wellstood, C.J. Lobb, R.S. Newrock, and M.G. Forrester, *Phys. Rev. B* **62**, 14 380 (2000).
- ²⁸T. Hasegawa (private communication).
- ²⁹D.J. Miller, V.R. Todt, M.St. Louis-Weber, X.F. Zhang, D.G. Steel, M.B. Field, and K.E. Gray, *Mater. Sci. Eng.*, **B 53**, 125 (1998); M.St. Louis-Weber, V.P. Dravid, V.R. Todt, X.F. Zhang, D.J. Miller, and U. Balachandran, *Phys. Rev. B* **54**, 16 238 (1996); D. Miller (private communication).
- ³⁰H. Hilgenkamp and J. Mannhart, *Appl. Phys. Lett.* **73**, 265 (1998).
- ³¹Yu. Eltsev, K. Nakao, Y. Yamada, Y. Takahashi, J. G. Wen, I. Hirabayashi, Y. Enomoto, and N. Koshizuka, The 2000 International Workshop on Superconductivity, Shimane, Japan, 2000, pp. 41–43.
- ³²H. Hilgenkamp, J. Mannhart, and B. Mayer, *Phys. Rev. B* **53**, 14 586 (1996).
- ³³K. Gorny, O.M. Vyaselev, J.A. Martindale, Y.A. Nandor, C.H. Pennington, P.C. Hammel, W.L. Hults, J.L. Smith, P.L. Kuhns, A.P. Reyes, and W.G. Moulton, *Phys. Rev. Lett.* **82**, 177 (1999); K. Gorny (private communication).
- ³⁴G.-q. Zheng, W.G. Clark, Y. Kitaoka, K. Asayama, Y. Kodama, P. Kuhns, and W.G. Moulton, *Phys. Rev. B* **60**, R9947 (1999).
- ³⁵V.V. Kabanov, J. Demsar, B. Podobnik, and D. Mihailovic, *Phys. Rev. B* **59**, 1497 (1999).
- ³⁶H.F. Fong, P. Bourges, Y. Sidis, L.O. Regnault, J. Bossy, A. Ivanov, D.L. Milius, I.A. Aksay, and B. Keimer, *Phys. Rev. Lett.* **82**, 1939 (1999); Y. Sidis, P. Bourges, H.F. Fong, B. Keimer, L.P. Regnault, J. Bossy, A. Ivanov, B. Hennion, P. Gautier-Picard, G. Collin, D.L. Milius, and I.A. Aksay, *ibid.* **84**, 5900 (2000).
- ³⁷R.A. Klemm, *Physica C* **341-348**, 839 (2000).
- ³⁸Y. Zhu, Q. Li, Y.N. Tsay, M. Suenaga, G.D. Gu, and N. Koshizuka, *Phys. Rev. B* **57**, 8601 (1998); Y. Zhu, L. Wu, J.Y. Wang, Q. Li, Y.N. Tsay, and M. Suenaga, *Microsc. Microanal.* **3**, 423 (1997).
- ³⁹J.-L. Wang, X.Y. Cai, R.J. Kelley, M.D. Vaudin, S.E. Babcock, and D.C. Larbalestier, *Physica C* **230**, 189 (1994).
- ⁴⁰R.A. Klemm, C.T. Rieck, and K. Scharnberg, *Phys. Rev. B* **61**, 5913 (2000); *ibid.* **58**, 1051 (1998).
- ⁴¹G. Arnold and R.A. Klemm, *Phys. Rev. B* **62**, 661 (2000).
- ⁴²S. Massida, J. Yu, and A.J. Freeman, *Physica C* **152**, 251 (1988).
- ⁴³C.G. Olson, R. Liu, D.W. Lynch, R.S. List, A.J. Arko, B.W. Veal, Y.C. Chang, P.Z. Jiang, and A.P. Paulikas, *Phys. Rev. B* **42**, 381 (1990).
- ⁴⁴R. Kleiner and P. Müller, *Phys. Rev. B* **49**, 1327 (1994).
- ⁴⁵A. Bille, C. T. Rieck, and K. Scharnberg, in *Symmetry and Pairing in Superconductors*, edited by M. Ausloos and S. Kruchinin, (Kluwer, Dordrecht, 1999), pp. 231–244.
- ⁴⁶A.I. Liechtenstein, O. Gunnarsson, O.K. Andersen, and R.M. Martin, *Phys. Rev. B* **54**, 12 505 (1996); S.Y. Savrasov and O.K. Andersen, *Phys. Rev. Lett.* **77**, 4430 (1996); O. Jepsen, O.K. Andersen, I. Das Gupta, and S.Y. Savrasov, *J. Phys. Chem. Solids* **59**, 1718 (1998); O.K. Andersen, S.Y. Savrasov, O. Jepsen, and A.I. Liechtenstein, *J. Low Temp. Phys.* **105**, 285 (1996).
- ⁴⁷T. Xiang and J.M. Wheatley, *Phys. Rev. Lett.* **77**, 4632 (1996).
- ⁴⁸We remark that the terminology is a bit different than some, as our “anomalous-*s*-wave” OP has often been referred to as an “extended-*s*-wave” OP.
- ⁴⁹P. Monthoux and D. Pines, *Phys. Rev. Lett.* **69**, 961 (1992); *Phys. Rev. B* **47**, 6069 (1993).
- ⁵⁰T. Dahm, J. Erdmenger, K. Scharnberg, and C.T. Rieck, *Phys. Rev. B* **48**, 3896 (1993).
- ⁵¹G. Santi, T. Jarlborg, M. Peter, and M. Weger, *Physica C* **259**, 253 (1996).
- ⁵²A. Bille and K. Scharnberg, *J. Phys. Chem. Solids* **59**, 2110 (1998).
- ⁵³M.J. Graf, M. Palumbo, D. Rainer, and J.A. Sauls, *Phys. Rev. B* **52**, 10 588 (1995); M.J. Graf, D. Rainer, and J.A. Sauls, *ibid.* **47**, 12 089 (1993).
- ⁵⁴W. Kim and J.P. Carbotte, *Phys. Rev. B* **61**, R11 886 (2000).
- ⁵⁵A.G. Rojo and K. Levin, *Phys. Rev. B* **48**, 16 861 (1993).
- ⁵⁶R.J. Radtke, V.N. Kostur, and K. Levin, *Phys. Rev. B* **53**, R522 (1996).
- ⁵⁷R.A. Klemm, A. Bille, C.T. Rieck, K. Scharnberg, and G. Arnold, *J. Low Temp. Phys.* **117**, 509 (1999); R.A. Klemm, G. Arnold, A. Bille, and K. Scharnberg, *Physica C* **341-348**, 1663 (2000); A. Bille, R.A. Klemm, and K. Scharnberg, cond-mat/0005288 (unpublished).
- ⁵⁸S. Tajima, G.D. Gu, S. Miyamoto, A. Odagawa, and N. Koshizuka, *Phys. Rev. B* **48**, 16 164 (1993).
- ⁵⁹K. Tamasaku, Y. Nakamura, and S. Uchida, *Phys. Rev. Lett.* **63**, 422 (1989).
- ⁶⁰D.N. Basov, S.I. Woods, A.S. Katz, E.J. Singley, R.C. Dynes, M. Xu, D.G. Hinks, C.C. Homes, and M. Strongin, *Science* **283**, 49 (1999).
- ⁶¹S. Tajima, J. Schützmann, S. Miyamoto, I. Teraskai, Y. Sato, and R. Hauff, *Phys. Rev. B* **55**, 6051 (1997).
- ⁶²S. Katz, S.I. Woods, E.J. Singley, T.W. Li, M. Xu, D.G. Hinks, R.C. Dynes, and D.N. Basov, *Phys. Rev. B* **61**, 5930 (2000).
- ⁶³E.J. Singley, A.S. Katz, S.I. Woods, R.C. Dynes, D.N. Basov, K.

- Kurahashi, and K. Yamada, Bull. Am. Phys. Soc. **45**, 887 (2000).
- ⁶⁴Yu.I. Latyshev, T. Yamashita, L.N. Bulaevskii, M.J. Graf, A.V. Balatsky, and M.P. Maley, Phys. Rev. Lett. **82**, 5345 (1999).
- ⁶⁵P.W. Anderson, Science **268**, 1154 (1995).
- ⁶⁶L.B. Ioffe and A.J. Millis, Phys. Rev. B **61**, 9077 (2000).
- ⁶⁷X.B. Kan and S.C. Moss, Acta Crystallogr., Sect. B: Struct. Sci. **48**, 122 (1992).
- ⁶⁸Y. Zhu (private communication).